Current Research (2013) Newfoundland and Labrador Department of Natural Resources
Geological Survey, Report 13-1, pages 167-188

GEOLOGICAL SETTING, GEOCHRONOLOGICAL CONSTRAINTS AND THE NATURE OF MINERALIZATION AT THE MOSQUITO HILL (HUXTER LANE) GOLD DEPOSIT, CENTRAL NEWFOUNDLAND

H.A. Sandeman, D.H.C. Wilton[1], J. Conliffe, T. Froude[2] and J.M. O'Driscoll[3]
Mineral Deposits Section
[1] Department of Earth Sciences, Memorial University, St. John's, NL, A1B 3X5
[2] Golden Dory Resources Ltd., P.O. Box 940, Bishop's Falls, NL, A0H 1C0
[3] Altius Minerals Corporation, Suite 202, 66 Kenmount Road, St. John's, NL, A1B 3V7

ABSTRACT

The Mosquito Hill gold deposit in NTS map area 2D/5 of central Newfoundland was discovered in 1998, through prospecting and sampling of arsenopyrite-bearing quartz-feldspar porphyry float, in extensive till cover, immediately south of the Northwest Gander River. This geologically complex area contains from northwest–southeast: Precambrian to Cambrian rocks of the Spruce Brook Formation of the Ganderian Mount Cormack Subzone; the Cambrian ophiolitic Coy Pond Complex and, the Cambrian to Ordovician marine sedimentary and volcanic rocks of the Baie D'Espoir Group. Exploration work and ongoing geoscientific investigations indicate that Mosquito Hill mineralization is mainly hosted in non-foliated, quartz-veined and sericite–arsenopyrite–pyrite-altered quartz-feldspar ± biotite ± hornblende-bearing, subvolcanic andesite–dacite porphyry (Mosquito Hill porphyry: MHP). The MHP ranges from fine to coarse grained and exhibits transitional contacts with compositionally similar crystal-lithic lapilli tuffs. The MHP is interleaved with affiliated volcaniclastic tuffs, epiclastic sandstones and grey and black graphitic shales and mudstones of the North Steady Pond Formation of the Baie d'Espoir Group, as well as a number of discrete mélange intervals. Mineralization consists of ≤15% disseminated euhedral arsenopyrite spatially associated with pyrite and abundant subhedral sericite grains and variable Fe-carbonate. Quartz veining appears to be slightly younger than alteration and highly anomalous gold is associated with abundant arsenopyrite rather than veining. Free gold has not been observed.

The LAM-ICP-MS U–Pb zircon geochronology for two samples indicates that the MHP crystallized during the interval 508–469 Ma (494 ± 14 and 477 ± 8 Ma); the younger date overlapping, within error, the only other dated felsic volcanogenic rock (Twillick Brook Member, 468 ± 2 Ma), exposed in the easternmost Exploits Subzone. An intermediate dyke that crosscuts a portion of the mélange below mylonitized MHP yielded an age of 464 ± 7 Ma, placing a lower limit on the age of the volcanic rocks of the North Steady Pond Formation and demonstrating that some of the mélange must have formed in the Ordovician. Randomly oriented sericite, forming part of the alteration assemblage in the MHP yielded two identical Devonian ^{40}Ar–^{39}Ar plateau ages of 406 ± 2 Ma. As these rocks preserve sub-greenschist-facies metamorphic mineral assemblages, the hydrothermal fluids generating the mineralization at Mosquito Hill must have immediately postdated regional widespread Silurian emplacement of bimodal granitoid intrusions and metamorphism and deformation in the Hermitage Flexure to the southwest.

INTRODUCTION

The Mosquito Hill (Huxter Lane) gold deposit is located ~50 km south of Grand Falls-Windsor, Newfoundland in the Burnt Hill map area (NTS 2D/5; Figure 1). Access to the property is *via* the now disused Little Gull River Resource Road. Prior to the construction of the Bay d'Espoir Highway in the early 1970s and systematic 1:50 000-scale geological mapping in the early 1980s, little exploration or academic work had been completed. For a complete summary of historical investigations prior to 1985, the reader is referred to Colman-Sadd (1985) and all subsequent scientific work is summarized in Colman-Sadd *et al*. (1992); Valverde-Vaquero *et al*. (2006); Zagorevski *et al.* (2007) and Sandeman *et al.* (2012).

Systematic mineral exploration for gold in the area began after the release of a regional lake-sediment compila-

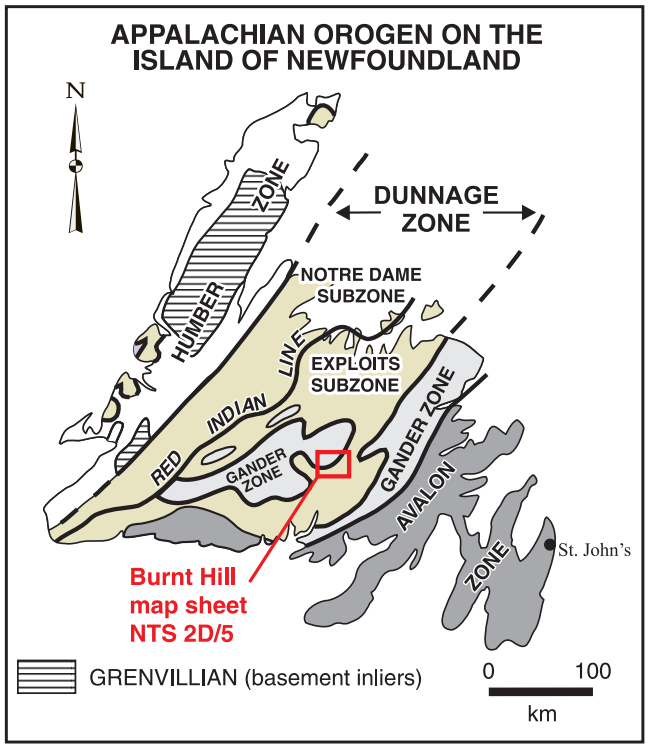

Figure 1. *Simplified geological map of Newfoundland showing the location of the Burnt Hill map area (NTS 2D/5), which hosts the Mosquito Hill gold deposit.*

tion (Davenport *et al.,* 1994), resulting in the discovery of mineralized porphyritic granitoid float in 1998, immediately south of the Northwest Gander River and west of the Bay d'Espoir Highway on the Huxter Lane Property (Quinlan and Quinlan, 1999). Since then, the area has seen increased exploration activity for gold. This exploration activity included detailed prospecting, soil and rock sampling and ground geophysics (IP: McVeigh, 2004; House, 2005); further ground geophysics (IP), trenching, mapping, and channel and soil sampling (House, 2006); the acquisition of detailed (75-m-line spacing) property-scale aeromagnetic geophysical data (House and Newport, 2007) and more recently extensive diamond drilling (House and Newport, 2007; House, 2008; Evans and Vatcher, 2009; Giroux and Froude, 2010; Evans, 2010). This report builds upon the geological observations and data of Colman-Sadd and Swinden (1984); Colman-Sadd (1985); Colman-Sadd *et al*. (1992) and Sandeman *et al*. (2012) and incorporates some recent mineral industry data (House and Newport, 2007; House, 2008; Evans and Vatcher, 2009; Giroux and Froude, 2010; Evans, 2010). Surface trenches and diamond-drill holes provide new information on lithological variability and rock-unit inter-relationships allowing for testable geological hypotheses.

This report presents a description of the nature and style of mineralization at Mosquito Hill and summarizes new field and petrographic observations. New laser ablation-inductively coupled plasma mass spectrometry (LAM-ICPMS), U–Pb geochronological and ^{40}Ar–^{39}Ar thermochronological data for mineralized and non-mineralized igneous rocks associated with the deposit are also presented and discussed. These data provide new constraints on the crystallization ages of the host rock-types as well as a minimum age for alteration of the host rock and accompanying gold deposition.

REGIONAL SETTING AND PREVIOUS WORK

The study area straddles the boundary between the Exploits Subzone of the Dunnage Zone, and the Mount Cormack Subzone, which is considered to represent part of the Gander Zone (Colman-Sadd and Swinden, 1984; Colman-Sadd *et al*., 1992: Figure 1). The Exploits Subzone consists of intra-oceanic arc and back-arc rocks that were formed along the eastern margin of Iapetus, proximal to the Ganderian, Gondwanan margin (*e.g*., van Staal, 1994; van Staal *et al*., 1998; Zagorevski *et al*., 2007). These were subsequently tectonically stacked and emplaced eastward over the Gander Zone margin during the Middle Ordovician Penobscot orogeny.

The region of central Newfoundland including the study area forms a peneplaned flatland having little topographical relief (*ca.* 130–250 m asl). The Mosquito Hill area includes a mature river system developed on thick hummocky terrain, ablation and basal till with local alluvium, bogs and concealed bedrock (Liverman and Taylor, 1990). Intact bedrock outcrop is very scarce, typically «1%. Very rare regional glacial-flow indicators are dominantly bi-directional, but local uni-directional straie indicate ice flow from the north to the south (Proudfoot *et al.,* 2005). Nevertheless, mapping of the sparse outcrop has enabled a basic understanding and subdivision of the geology of the area (Blackwood, 1982; Colman-Sadd, 1985; Colman-Sadd and Russell, 1988).

From northwest to southeast, the area encompasses the southeastern margin of the elliptical Mount Cormack Subzone, the ophiolitic rocks of the Coy Pond and Great Bend complexes and, the felsic volcanic, volcaniclastic and fine-grained clastic sedimentary rocks of the Baie d'Espoir Group (Figure 2; Colman-Sadd, 1980, 1985). The rocks of the Mount Cormack Subzone proximal to the Mosquito Hill deposit comprise chlorite- to biotite-grade, decimetre- to metre-scale bedded blue-grey to black psammite and pelite

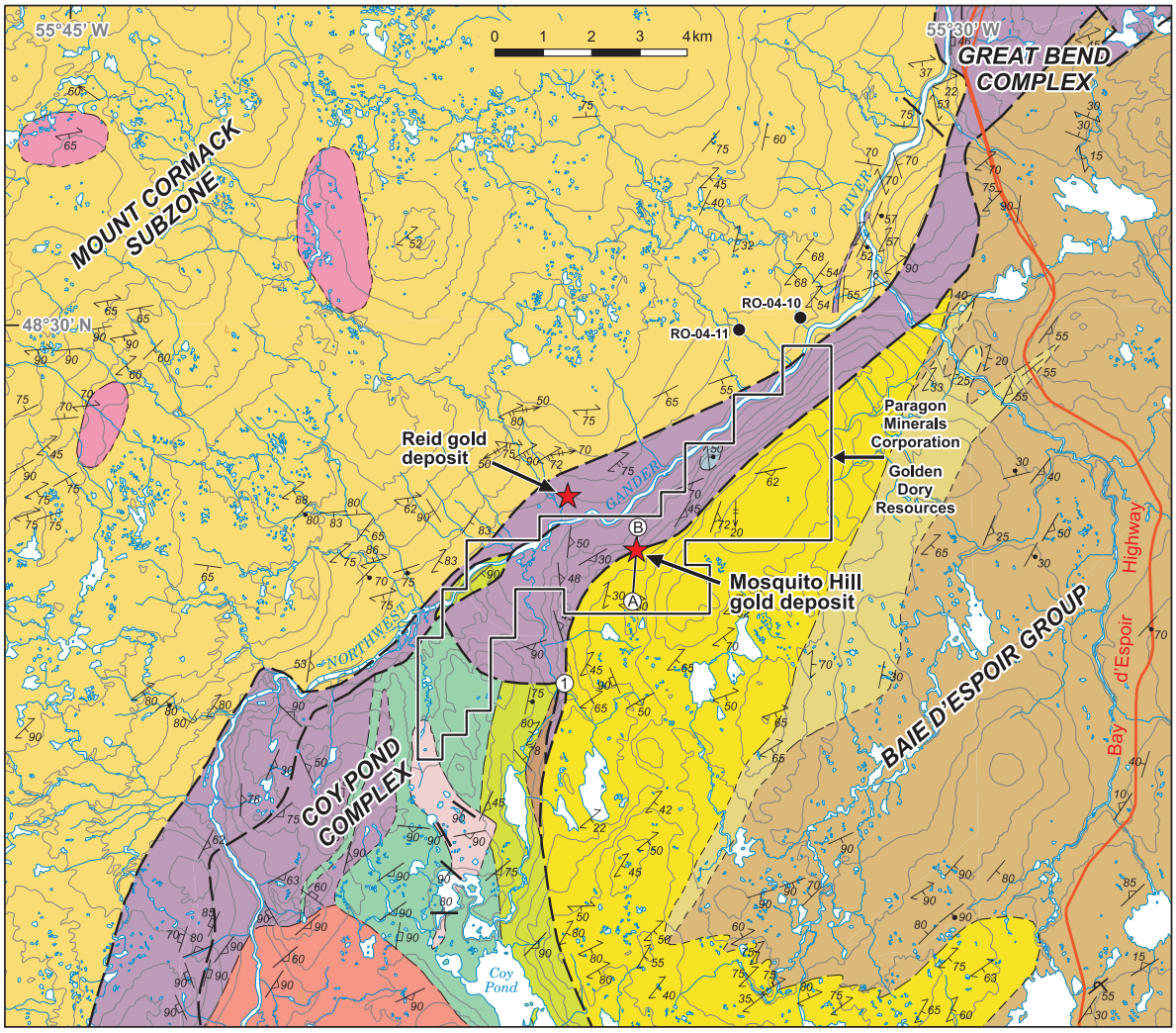

Figure 2. *Simplified geological map of the region around the Mosquito Hill and Reid gold deposits (adapted after Colman-Sadd, 1985). Note the location of the cross-section (A–B: Figure 5) and locality 1 as well as the close proximity to the Reid gold deposit (Sandeman* et al., *2012). Ages quoted in legend are from: 1) Colman-Sadd* et al. *(1992); 2) Sandeman* et al. *(2012) and; 3)* this study.

of the Spruce Brook Formation. These rocks pass gradationally northwestward into upper amphibolite-facies gneisses and metasedimentary diatexite, along with minor mafic intrusions and, the Middle Ordovician Through Hills granite ($464^{+4}/_{-3}$ Ma; Colman-Sadd, 1985; Colman-Sadd *et al*., 1992; Valverde-Vaquero *et al.,* 2006) that contains garnet + tourmaline + muscovite and is considered to be of anatectic origin. The contact between the metasedimentary rocks of the Mount Cormack Subzone and the Coy Pond Complex is not exposed, but on the basis of regional aeromagnetic data is inferred to lie immediately to the north of, and likely at depth below the adjacent Reid gold deposit (Figure 2; Colman-Sadd, 1985; Dimmell, 2003, 2004; Evans *et al*., 2007; Sandeman *et al.*, 2012). North of the Northwest Gander River, a likely structural break between southeast-dipping ultramafic schists and structurally underlying sedimentary rocks has been noted in two industry drillholes (Figure 2, RO-04-10 and 11). The low-grade, black argillitic sedimentary rocks intersected in these drillholes differ, however, from typical Spruce Brook Formation turbidites (Dimmell, 2004; D. Evans, personal communication, 2012).

The quartz-rich, blue-grey turbiditic sedimentary rocks of the Spruce Brook Formation have been correlated with rocks of the Gander Group of the Gander Zone (Colman-Sadd, 1985; Williams *et al.,* 1988). The age of the Spruce Brook Formation is not constrained, but is considered to be Precambrian to Early Ordovician based on this correlation (Colman-Sadd *et al*., 1992). Colman-Sadd (1985) and Dec and Colman-Sadd (1990) proposed a Middle Ordovician age for a brachiopod-bearing limestone conglomerate that was interpreted to form part of the Spruce Brook Formation; however, the critical contacts between this conglomerate and other units are not exposed and its precise stratigraphic relationships are not known.

Southeast of the rocks of the Mount Cormack Subzone and underlying the Northwest Gander River lowlands are the rocks of the Coy Pond and Great Bend complexes (Colman-Sadd, 1982, 1985; Colman-Sadd and Russell, 1988; Colman-Sadd *et al*., 1992; Dimmell *et al.*, 2003, Dimmell, 2004; Evans *et al.*, 2007; Evans, 2010, 2011; Sandeman *et al.,* 2012). North of Coy Pond (Figure 2), a fault disrupted, but nevertheless almost complete ophiolite stratigraphy is preserved with peridotites exposed in the west and mafic dykes, lavas and sedimentary rocks exposed in the east. In the east, mafic pillow lavas that are observed to grade transitionally into diabase and gabbro are unconformably overlain by a unit of thin-bedded black argillite, sandstone and polymict conglomerate (Colman-Sadd, 1985). Graptolites retrieved from the argillite portion of this unit were determined to be *Undulograptus austrodentatus* (*s.l.*) occurring with the trilobite fauna *Cyclopyge grandis brevirhachis*. This fauna is interpreted to indicate an Early Ordovician (Tremadocian to Floian: International Chronostratigraphic Chart; www.stratigraphy.com) age and to have Gondwanan rather than Laurentian affinities (Williams *et al*., 1992). Altered trondhjemite forms a large irregular intrusion that crosscuts gabbro and diabase, but is itself cut by mafic dykes. Gabbro and diabase pass gradationally westward into massive and layered pyroxenite, wehrlite and intermixed gabbro. These units are separated from a thick basal harzburgite by a thin unit of strongly sheared serpentinite and talc–magnesite schist. To the northeast, the ophiolite complex tapers into a narrow (~1 km wide) zone of brecciated and sheared peridotite. Prior to industry trenching, the contact between the rocks of the Coy Pond Complex and the volcanic and volcaniclastic sedimentary rocks of the North Steady Pond Formation of the Baie d'Espoir Group was exposed only at one locality, in a brook 3 km east of Huxter Pond (Colman-Sadd, 1985; locality 1, Figure 2). There, Colman-Sadd (*op. cit*.) described a zone of sheared serpentinite defining an east-dipping reverse fault between the Coy Pond Complex and the Baie D'Espoir Group. Industry trenching has now exposed two more examples of this contact zone (House, 2005). The ophiolitic rocks are very poorly exposed and their outcrop patterns have been largely inferred from subcrop, fluvioglacial float and regional aeromagnetic data. Geological contacts are, with few exceptions, everywhere inferred.

South and east of the Coy Pond Complex are clastic sedimentary, volcaniclastic and volcanic rocks of the North Steady Pond Formation (Figure 2; Colman-Sadd, 1980, 1985). The thickness and internal stratigraphy of the formation are not known because of the poor exposure as well as a lack of marker intervals and the presence of tight to isoclinal folds. From north to south, the rocks include felsic volcanic flows and subvolcanic intrusions, tuffs and volcaniclastic sandstones (also termed the Huxter volcanic belt; Colman-Sadd and Swinden, 1982); a discontinuous interval of clast-supported polymict conglomerate containing argillite, siltstone, psammite, chert and felsic and mafic volcanic clasts and, thick interbedded sequences of thin- and medium-bedded arkosic sandstone, siltstone and phyllite (Figure 2). Intermediate to felsic, subvolcanic quartz + feldspar porphyritic rocks host the mineralization at the Mosquito Hill deposit.

The rocks of the Baie D'Espoir Group display characteristics more akin to those of the Exploits Subzone of the Dunnage Zone. The black to grey shale of the region contain Middle to Late Ordovician graptolite assemblages (Caradocian, Sandbian to Katian: International Chronostratigraphic Chart; www.stratigraphy.com) that have Gondwanan affinities (Williams, 1991), indicating that they must have formed proximal to the Gondwanan eastern margin of Iapetus. On the basis of regional correlations, Colman-Sadd and

Swinden (1984) and Colman-Sadd (1985) proposed that the Mount Cormack Subzone represents Gander Zone rocks exposed in an upward-domed basement window, encircled by a structurally modified, tectonic klippe of 'Penobscot' arc ophiolites and their sedimentary cover. The Cambrian (*ca*. 510 to 494 Ma; Dunning and Krogh, 1985; Sandeman *et al*., 2012) intra-oceanic and continental-arc and back-arc assemblages of the eastern Dunnage Zone were thrust eastward (present-day coordinates) over the Gander Zone margin (Colman-Sadd *et al*., 1992; van Staal *et al*., 1998; Zagorevski *et al.,* 2007). The coincidence in the age of metamorphism and accompanying anatexis in the Mount Cormack window at *ca*. 464 Ma with the intrusion of the Ordovician Partridgeberry Hills pluton ($464^{+6}/_{-4}$ Ma) across the Exploits–Gander subzone boundary are interpreted to indicate that overthrusting of the Exploits oceanic tract, over the Gander Zone, was finished by that time (Colman-Sadd *et al.,* 1992; Valverde-Vaquero *et al*., 2006). The cause of younger, normal faulted contacts between the Coy Pond Complex and the sedimentary rocks of the Mount Cormack window and the North Steady Pond Formation, as well as second-generation fabrics in the southern portions of the Partridgeberry Hills pluton and in the adjacent Baie D'Espoir Group, was described as uncertain. These faults and fabrics were suggested to have resulted from further crustal shortening or perhaps forceful intrusion of the semi-solidified Partridgeberry Hills granitic intrusion. Thus, the extent of, and indeed the existence of Silurian (Salinic) or Devonian (Acadian) orogenic effects in the region, have been downplayed by all investigators.

GEOLOGY OF THE MOSQUITO HILL DEPOSIT

Outcrop and subcrop exposures in, and around, the vicinity of Mosquito Hill (Figure 2) are very rare and the few exposures comprise thick-bedded volcaniclastic quartz arenite, dacitic, volcaniclastic and subvolcanic intrusive rocks and, variably tectonized black graphitic shale (Colman-Sadd, 1985; Colman-Sadd *et al*., 1992). Detailed mapping, trenching and drilling at the Mosquito Hill deposit (MacVeigh, 2004; House, 2006; House and Newport, 2007; House, 2008; Evans and Vatcher, 2009; Evans, 2010) provide new bedrock exposures that reveal important lithological relationships and orientations.

SLOPE TRENCH

The Slope trench is one of 4 trenches excavated on the property by Paragon Minerals Corporation (House, 2005) that exposed mineralized bedrock. It is a ~60-m-long, linear, southeast–northwest-trending trench that exposes the contact zone (Figure 3) between variably quartz-veined, sericite–pyrite–arsenopyrite-carbonate-altered dacite porphyry (Mosquito Hill porphyry: MHP; Plate 1) in the structural hanging wall with a composite unit in the footwall (Figure 3). The composite unit contains millimetre- to metre-scale clasts of polymict conglomerate, serpentinized ultramafic rocks, grey shale, fine-grained variably coloured sandstones and sericite-altered quartz-feldspar porphyritic clasts, all disposed in sinuous bands of a strongly foliated

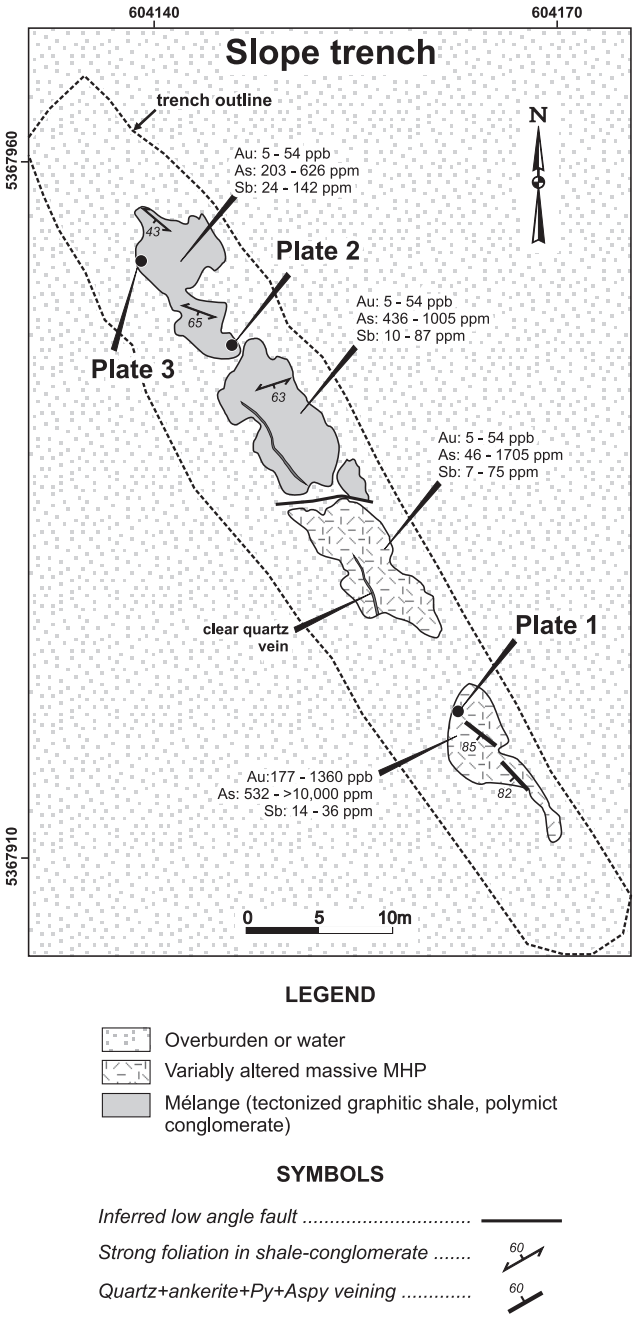

Figure 3. *Geological map of the Slope trench showing the disposition of units as well as the ranges in channel-sample assay values for gold, arsenic and antimony (House, 2005). Channel samples ranged in length from 0.25 to 1.05 m long.*

Plate 1. *Quartz–ankerite-veined, massive, fine- to medium-grained, tan–orange-weathering Mosquito Hill porphyry from the Slope trench. Location is given in Figure 3. This intersection yielded an assay of ~250 ppb Au. The pen is 14 cm in length.*

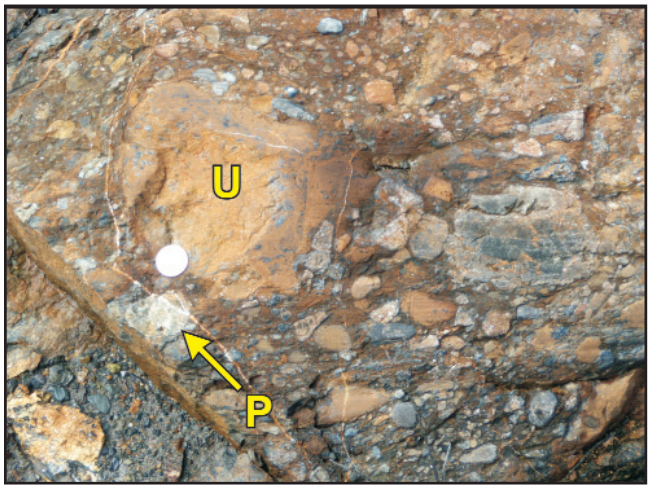

Plate 2. *Polymict conglomerate forming part of the mélange unit in the structural footwall of the mineralized porphyry in the Slope trench. Note the large ultramafic clast (U) as well as the pale, bleached quartz-feldspar porphyry clast (P). A proximal sample of this rock yielded an assay of < 5 ppb Au. Location is given in Figure 3. The $2 coin is 28 mm in diameter.*

graphitic black shale matrix (Plate 2). This unit closely resembles the non-genetic definition of an ophiolitic mélange (Silver and Beutner, 1980; Festa *et al*., 2012), derived from sub-aqueous erosion of adjacent or exotic rock-units during uplift, and associated with tectonic emplacement of the oceanic rocks over others. Shale lenses in the mélange locally exhibit intense strain and contain abundant discontinuous, dismembered and or folded quartz-carbonate veins (Plate 3). Channel samples obtained by Paragon Minerals Corporation (House, 2005) indicate that the mélange contains only weakly anomalous gold (≤54 ppb

Plate 3. *Chaotically foliated and folded quartz-veined black graphitic shale forming part of the mélange unit in the structural footwall of the mineralized porphyry in the Slope trench. Adjacent shale yielded an assay of < 5 ppb Au. Location is given in Figure 3. The $2 coin is 28 mm in diameter.*

Au), whereas the Mosquito Hill porphyry, particularly where intensely altered, exhibits more highly anomalous Au concentrations (≤1360 ppb Au). High concentrations of gold are correlated with elevated As concentrations and the occurrence of abundant disseminated arsenopyrite laths (≤2 mm). It is noteworthy that both the Mosquito Hill porphyry as well as the mélange unit have very strongly elevated antimony concentrations ranging from 7 to 75 ppm and 10 to 142 ppm Sb, respectively. These range from 7 to 355 times the average concentration of Sb in the crust (0.1 to 0.4 ppm Sb: Rudnick and Gao, 2003).

CONTACT TRENCH

The Contact trench is a ~60-m-long, sinuous but generally east-southeast-trending trench that exposes the same contact zone (Figure 4) between variably quartz-veined, sericite–pyrite–arsenopyrite-carbonate-altered Mosquito Hill porphyry in the structural hanging wall, and the composite mélange unit in the footwall. The mélange unit is essentially the same as that exposed in the Slope trench, however, the proportion of cobble- to pebble-sized ultramafic clast-bearing conglomerate is significantly greater in the Contact trench. The adjacent Mosquito Hill porphyry is generally massive, but is everywhere moderately to strongly sericite–pyrite–arsenopyrite-carbonate-altered and is variably quartz veined, with the greatest vein density at the eastern end. Channel samples (Paragon Minerals Corporation; House, 2005) indicate that although the mélange contains generally anomalous Au (≤588 ppb Au), the Mosquito Hill porphyry, particularly where strongly altered, contains more gold (≤4686 ppb Au) and, in particular, abundant euhedral arsenopyrite grains.

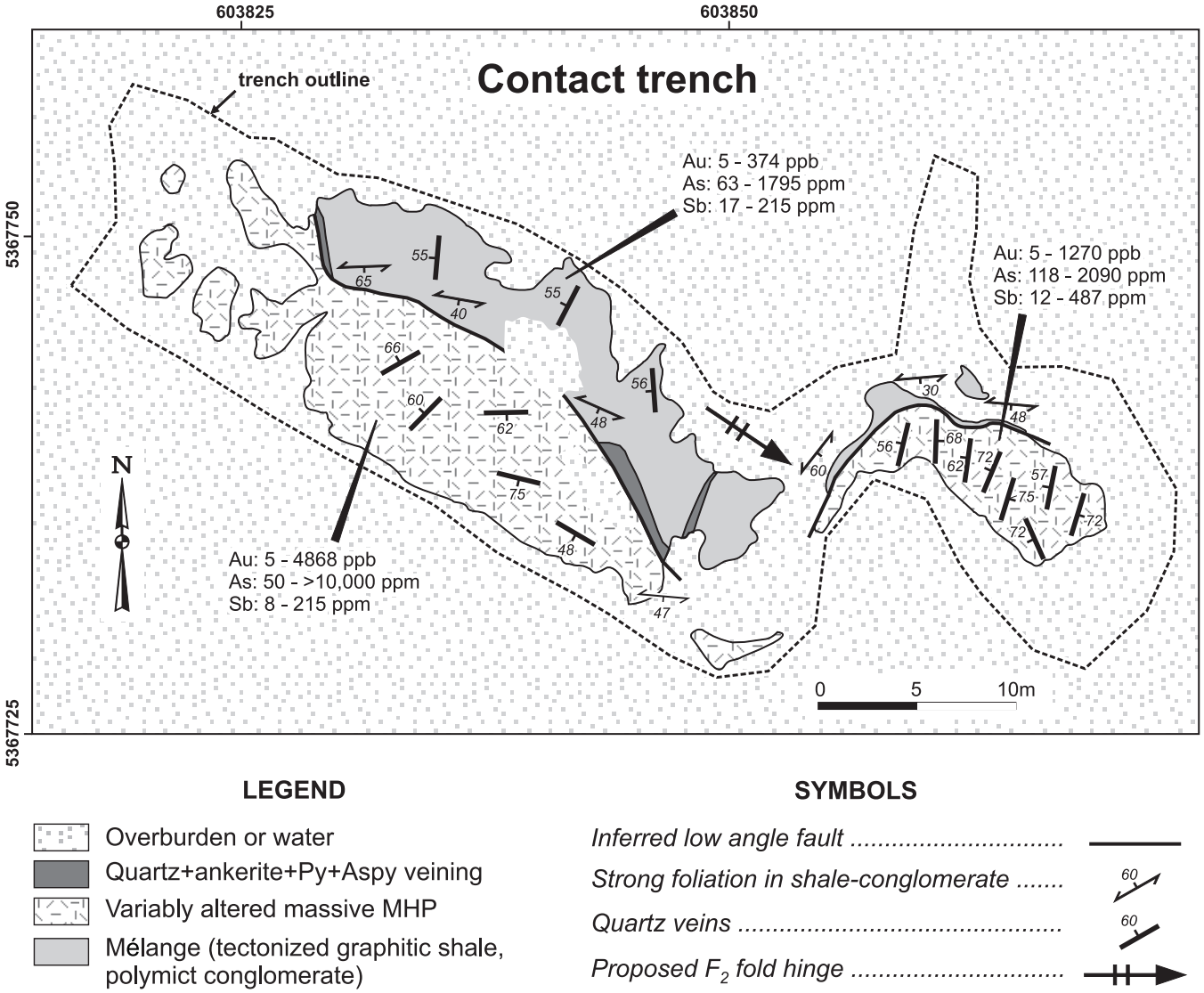

Figure 4. *Geological map of the Contact trench showing the disposition of units as well as the ranges in channel-sample assay values for gold, arsenic and antimony (House, 2005). Channel samples ranged in length from 0.25 to 1.05 m long.*

The sinuous form-surface of the schistose contact zone between the mélange and the Mosquito Hill porphyry dips moderately (~50°) to the south and east. If the sinuous nature of the contact represents a fold, then it is an approximately 20 m wavelength, S-asymmetric fold of the contact zone (Figure 4). If this is the case, then such an asymmetry indicates that it may be a parasitic fold associated with a major, map-scale, synformal closure of the stratigraphy to the southwest. Such a geometry is also suggested by the map-scale pattern of the Baie D'Espoir Group (Colman-Sadd, 1985) and the high-resolution (75-m-line spacing) aeromagnetic data obtained on the property by Paragon Minerals Corporation (House and Newport, 2007). The schistose and highly strained character of the shale below the contact in both trenches, and the fact that it appears to represent an ophiolitic mélange, suggest that the contact zone represents a fault, likely a thrust or reverse fault as suggested by Colman-Sadd (1985).

DIAMOND-DRILL HOLE DATA

A review of industry assessment reports, examination of their contained drillhole data logs, a detailed re-examination of one drillhole (HX06-16, House, 2005) along with selective examination and sampling of 3 other drillholes (HX09-33, HX10-53 and HX11-66, Evans and Vatcher, 2009; Evans, 2010) has been undertaken. These data allow construction of a schematic cross-section presenting a simplified tectonostratigraphy for the host geology of the deposit area (Figure 5; adapted after House and Newport,

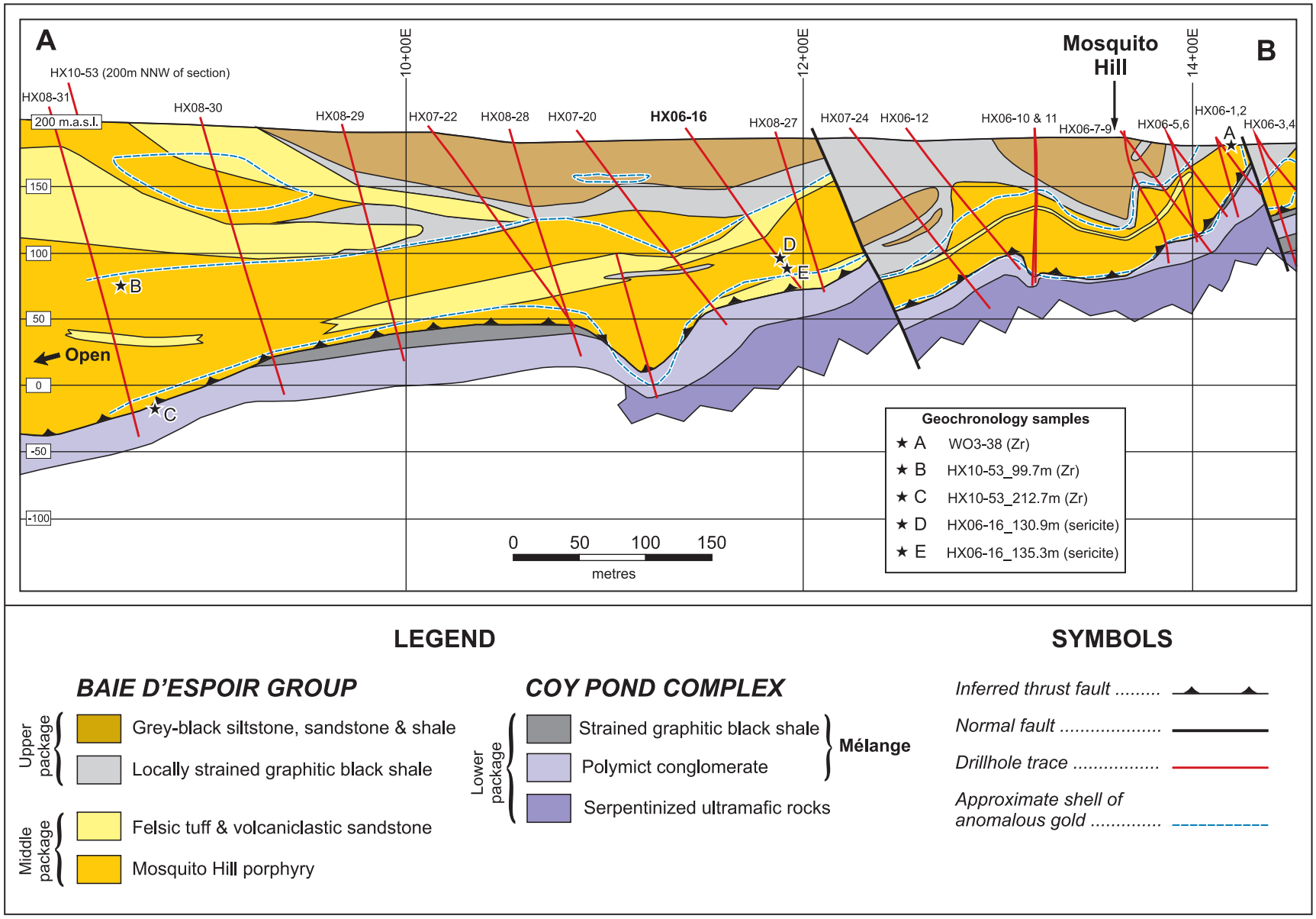

Figure 5. *Longitudinal cross-section (looking west-northwest) through the Coy Pond Complex–North Steady Pond Formation contact zone, as constructed from trench and drillhole data (House, 2006; House and Newport, 2007; Evans and Vatcher, 2009; Evans, 2010; Giroux and Froude, 2010) on the Mosquito Hill property. Note that there are at least two distinct black shale associations. The location of geochronological samples are indicated. Adapted from Giroux and Froude (2010).*

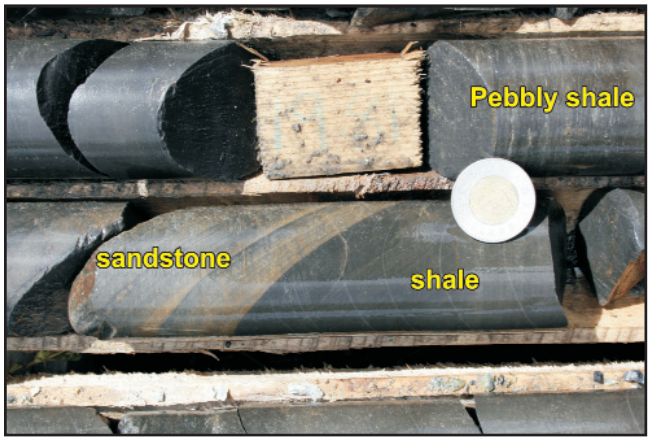

Plate 4. *Fine-grained grey-black shale and pebbly shale with fine-grained tan-grey sandstone intervals of the upper lithological package (HX06-16_19.8 m). The $2 coin is 28 mm in diameter.*

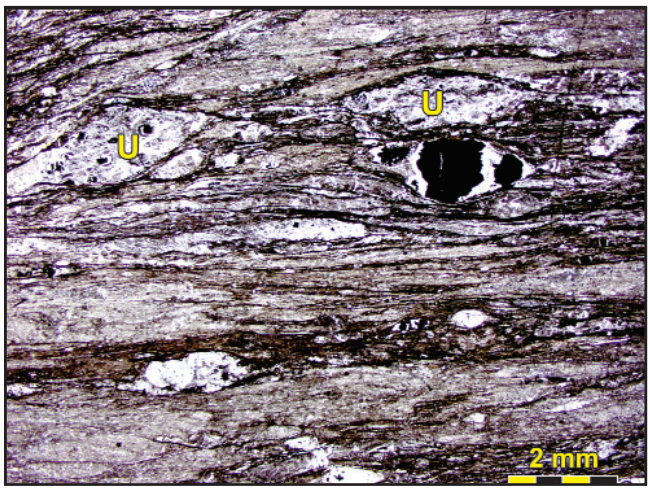

Plate 5. *Photomicrograph of a strongly foliated graphitic black shale (HX06-16_67.1 m) with flattened serpentinized ultramafic clasts (U) having remnant chromite grains.*

2007; House, 2008; Evans and Vatcher, 2009; Evans, 2010; Giroux and Froude, 2010). The cross-section shows an overall stratigraphic geometry comprising a sequence of three stacked rock assemblages or packages. This comprises an upper package of clastic sedimentary rocks of the North Steady Pond Formation; a middle package containing the Mosquito Hill porphyry and its volcanic and volcaniclastic carapace and; a lower package consisting of an ophiolitic mélange overlying a thick section of intact ultramafic rocks. These three assemblages may be clearly noted in many of the deep drillholes on the property (Figure 5).

In drillhole HX06-16 (Figure 5), thick alluvium or till (≤15 m) passes downhole into ~28 m of decimetre-scale bedded grey to black siltstone (Plate 4). No assay samples

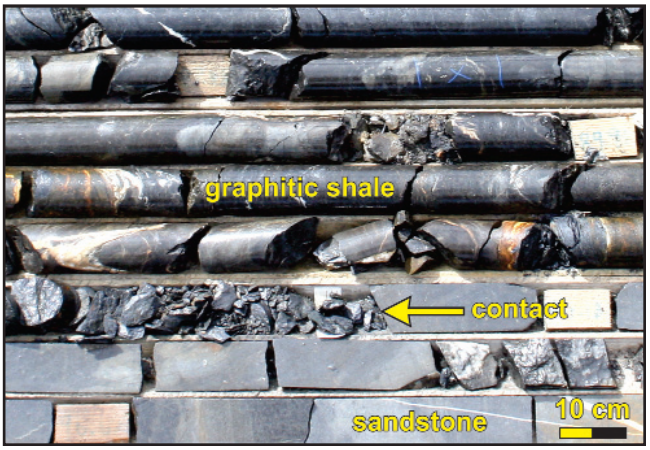

Plate 6. *Contact zone between strongly foliated graphitic black shale of the upper package with locally bedded volcanogenic sandstone and crystal tuff of the central package (HX06-16_94 m). Sandstone/tuff below the contact yielded assays of <300 ppb Au.*

were taken for this interval. This passed downward into 15 m of fine-grained, grey-tan sandstone and sparse shale intervals and rip-up clasts. This interval yielded 1-m-length assays of 13 to 299 ppb Au. Below the sandstone was a 28-m-thick interval of graphitic black shale that was not assayed. This graphitic, pebbly black shale interval is typically strongly schistose (Plate 5) and preserves brecciated and dismembered veins of quartz and calcite as well as serpentine clasts. These rocks comprise the upper lithostratigraphic package (Figure 5). The lower contacts of this package with the volcaniclastic sedimentary rocks and the Mosquito Hill porphyry are sharp, characterized by rubbly gouge-like graphitic shale and foliated more competent volcaniclastic sedimentary rocks (Plate 6).

Below the upper package of siliciclastic rocks is a second package containing a ≤60-m-thick sequence of quartz-feldspar crystal-lithic tuff and mineralogically similar volcaniclastic sandstones intruded by, and grading laterally into, the quartz + feldspar ± biotite ± hornblende porphyritic Mosquito Hill porphyry intrusion that is variably sericite–quartz-carbonate-altered and hosts most of the gold mineralization (Plate 7). Immediately below the abrupt contact with the overlying graphitic shale, ~20 m of a weakly altered quartz porphyritic tuff yielded 1-m-length assays of 19 to 305 ppb Au. The tuff grades into ~35 m of extensively sericite-carbonate-altered, quartz-veined and arsenopyrite-mineralized quartz-feldspar porphyry that yielded 1-m-length gold assays ranging from 383 to 5173 ppb Au. Typically, the porphyry is massive and medium grained (≤4 mm), but locally may exhibit layering, grading, crystal shards and lithic fragments. It varies from dark green to light apple-green and is variably altered, silicified, chloritized

Plate 7. *Medium-grained, tan-grey, quartz–ankerite-veined and sericite–arsenopyrite–pyrite-altered Mosquito Hill porphyry (HX06-16_117 m). This sample yielded an assay of 788 ppb Au.*

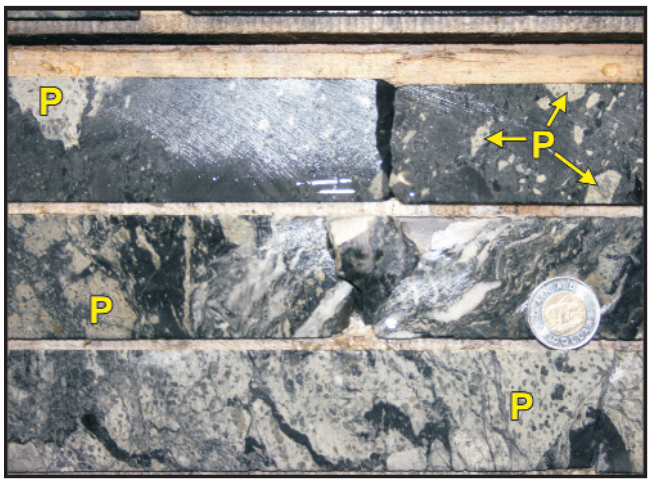

Plate 8. *Abundant clasts of bleached quartz-feldspar porphyritic volcanic clasts locally containing subhedral arsenopyrite and pyrite grains in the polmict conglomerate-mélange unit of the lowest package (HX10-53_213.5 m). P = quartz-feldspar porphyry clasts.*

and sericitized. Widespread, fine Fe-carbonate alteration affects much of the porphyry, the felsic tuff and locally, the intercalated volcanogenic sandstones.

Below the Mosquito Hill porphyry is an abrupt contact zone underlain by a >15 m interval of mélange defined by a chaotic and structurally disrupted sequence of typically strongly foliated, intimately intermixed black shale, serpentinized ultramafic blocks and polymict conglomerate (Plate 8) of the lowermost lithostratigraphic package. The polymict conglomerate contains a wide range of clast types including numerous sandstone types, serpentinized and talcose ultramafic rocks, abundant siltstone as well as porphyritic felsic volcanic clasts. Many of these clasts are

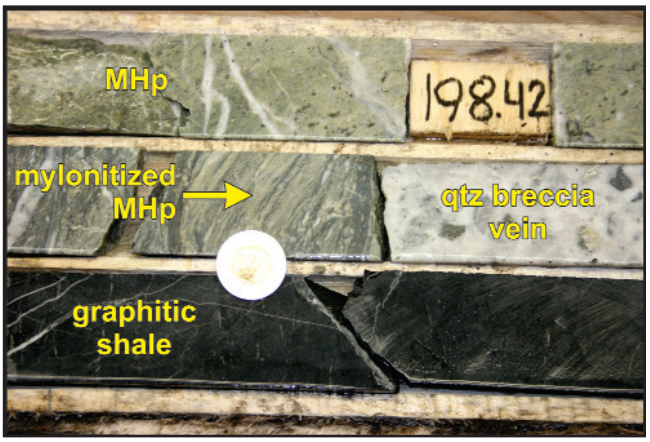

Plate 9. *Mylonitized base of the altered and mineralized Mosquito Hill porphyry in contact with a coarse quartz-breccia vein and deformed black shale in the structural footwall (HX10-53_200m). The mylonite yielded an assay of 3770 ppb Au. The $2 coin is 28 mm in diameter.*

sericite-carbonate-altered, arsenopyrite-mineralized quartz-feldspar porphyry that closely resembles the Mosquito Hill porphyry. Gold assays for this interval ranged from 5 to 69 ppb Au. In drillhole HX10-53 (over a ~1 m interval at its basal contact with the mélange (200 m depth)), the mineralized Mosquito Hill porphyry is transformed from massive porphyry into a ribbon mylonite (Plate 9). This lower lithological package mélange was first recognized in the Slope and Contact trenches (House, 2006; House and Newport, 2007; *see* above) where it similarly structurally underlies the mineralized porphyry. Interpretation of this unit was problematic and it was assigned a number of different names, including polymict conglomerate, black shale, graphitic black shale, sandstone, ultramafic conglomerate, ultramafic tuff and fragmental ultramafic unit (House and Newport, 2007; Evans and Vatcher, 2009; Evans, 2010). Deep drillholes (*e.g.*, HX06-9 or 24; Figure 5: House and Newport, 2007) penetrated massive, weakly deformed peridotite below the conglomerate–shale–ultramafic mélange intervals. Many of these intersections of mélange were noted to contain abundant clasts of altered porphyritic rock (Plate 10) containing arsenopyrite + pyrite mineralization (House and Newport, 2007: *e.g.,* DDH HX06-2_44 to 60 m or HX06-10_135 to 149 m; Figure 5).

Anomalous gold in drillcore, as in the trenches, is almost entirely hosted by the Mosquito Hill porphyry. The highest gold values are associated with the occurrence of disseminated euhedral laths of arsenopyrite. Although the abundant quartz veins do not appear to carry elevated gold values, they are spatially associated with a greater abundance of euhedral arsenopyrite in the adjacent porphyry. One-metre length core samples typically yielded from < 5 to 3500 ppb Au in the porphyry and typically <100 ppb in all

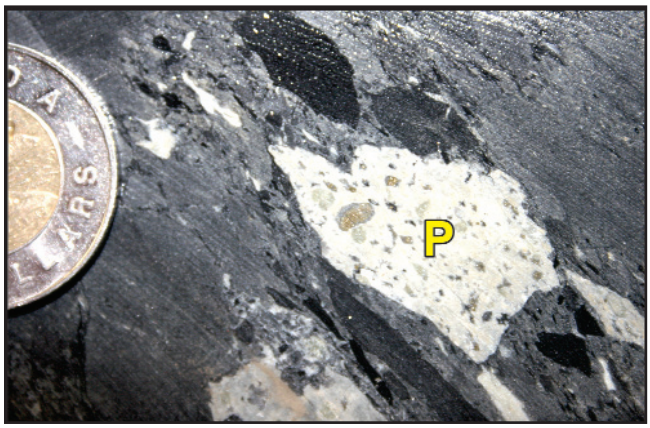

Plate 10. *Close-up of a massive, angular, bleached quartz-feldspar porphyritic clast (P) in the lower mélange unit (HX10-53_202 m). The $2 coin is 28 mm in diameter.*

other units (House, 2005; House and Newport, 2007). Gold is directly correlated with As, which ranges from 102 to >10 000 ppm in porphyry and 19 to 1275 ppm in other units. Gold mineralization is everywhere accompanied by strong sericite + carbonate alteration, discontinuous, typically narrow (≤25 cm) quartz veins and, abundant randomly dispersed subhedral pyrite and euhedral arsenopyrite (Plate 11A and B). Discrete gold grains have not yet been observed in samples of the Mosquito Hill porphyry.

GEOCHRONOLOGICAL SAMPLING

Samples for petrographic analysis and U–Pb and ^{40}Ar–^{39}Ar geochronology were obtained from the Slope, Contact and Main trenches (House, 2006) and also from 4 drillholes, including HX06-16 (House and Newport, 2007), one of the drillholes that yielded the most prospective Au intersections including 2.21 g/t Au over 35 m (up to 5173 ppb per metre). A large sample of quartz-plagioclase ± hornblende pophyritic Mosquito Hill porphyry (WO3-38) was obtained from the Main trench at Mosquito Hill (House, 2006) for LAM-ICPMS geochronology. This U–Pb data was first presented in a M.Sc. dissertation (O'Driscoll, 2006). To test the veracity of the data from WO3-38, a ~30 cm piece of quartz-plagioclase pophyritic Mosquito Hill porphyry in drillcore (sample HX10-53_99.7 m) was selected to compare with the earlier results (WO3-38). A third sample of drillcore from a dacitic dyke that crosscuts mélange immediately below mylonitized Mosquito Hill porphyry (W12-003: HX10-53_212.7 m) was obtained to help constrain the timing of formation of the mélange and provide a possible minimum age of volcanism in the North Steady Pond Formation.

Two samples of drillcore consisting of altered and mineralized quartz-plagioclase porphyritic dacite (HX06-16_130.9 m and HX06-16_135.3 m) were selected from the gold mineralized Mosquito Hill porphyry for ^{40}Ar–^{39}Ar thermochronology.

ANALYTICAL METHODS

The U–Pb age data for the Mosquito Hill porphyry were obtained using Laser Ablation ICP-MS (LAM-ICP-MS) analysis of zircon grains at the Department of Earth Sciences, Memorial University of Newfoundland (MUN). The samples were crushed and prepared using standard techniques including density separation using a Wilfley Table and heavy liquids using Methylene iodide followed by Franz magnetic separation and zircon grain picking in

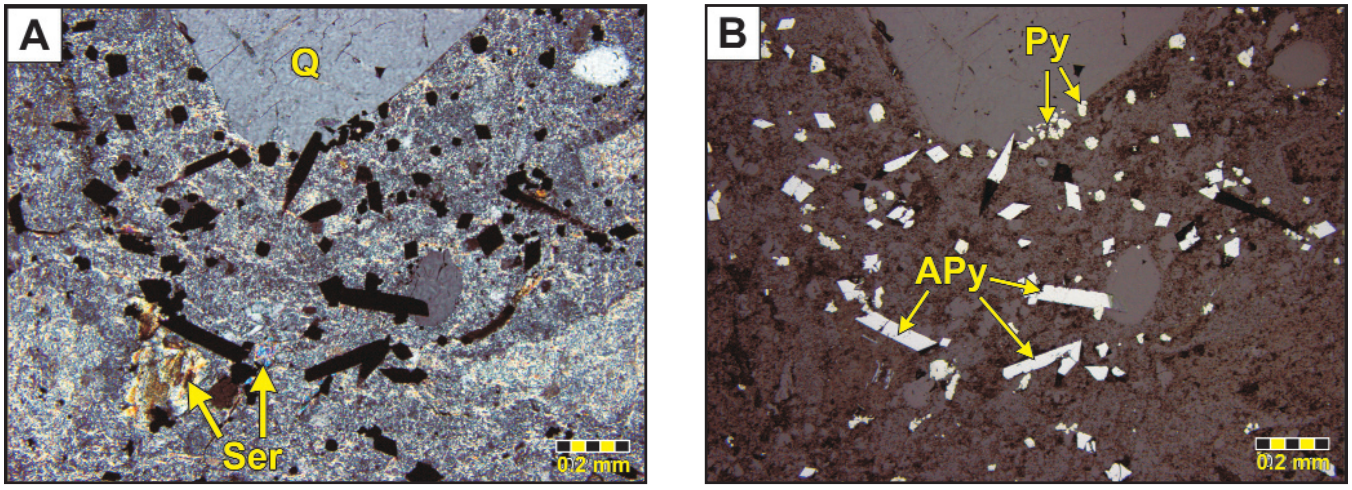

Plate 11. *A) Photomicrograph (crossed nicols) of the Mosquito Hill porphyry (HX06-16_131.25 m; 9380 ppb Au, 11972 ppm As, 20.6 ppm Sb). Large rounded quartz phenocrysts (Q) set in a fine-grained groundmass of disseminated sericite (Ser) and chlorite. Note the abundant disseminated euhedral arsenopyrite (APy) and pyrite (Py) and coarse sericite clumps. B) The same in reflected light.*

nanopure ethanol using a binocular microscope. The zircon grains were mounted in epoxy resin in a round ring assembly that was then polished and grains were subsequently analyzed using the LAM-ICP-MS. Details of the mass spectrometric method are described in detail by Kosler *et al.* (2002) and O'Driscoll (2006). The U–Pb data are presented in Table 1 and back-scattered electron images of representative analyzed zircon grains along with isochron plots are presented in Figures 6 to 8.

The ^{40}Ar–^{39}Ar age determinations were obtained at Queen's University ^{40}Ar–^{39}Ar Thermochronology Laboratory using the methods outlined in Minnett *et al.* (2012). The gas steps used in the calculation of the plateau ages are marked by asterisks in Table 2 and are shaded boxes in Figure 9. All age calculations used the ^{40}Ar–^{39}Ar age spectrum module of Ludwig (2003). The ^{40}Ar–^{39}Ar plateau ages are commonly defined by at least 3 contiguous gas release steps (consisting of >60% of released ^{39}Ar), with ^{40}Ar–^{39}Ar ages overlapping within error (McDougall and Harrison, 1988 and references therein; Snee *et al*., 1988; Singer and Pringle, 1996). The approximate argon closure temperatures for sericite (muscovite, *ca*. 350°C: McDougall and Harrison, 1988; Reynolds, 1992) are used to aid in the interpretation of the cooling history of the host rocks. Age uncertainties for all results are quoted at the 2σ uncertainty level and all concordia plots and diagrams show 2σ uncertainties.

U–Pb RESULTS

Approximately 40 zircon grains ranging in size from 40 by 40 µm to 50 by 120 µm were picked from sample WO3-38 and, in general, the grains were clear to very pale yellow and ranged from euhedral, needle like to equi-dimensional grains. A number of the smaller grains exhibit minor compositional zoning (Figure 6A). The LAM-ICP-MS analysis of 10 zircon crystals yielded a U–Pb zircon age of 494 ± 14 Ma (Table 1; Figure 6B). A number of grains yielded slightly younger (Pb-loss?) and slightly older (inheritance?) ages, however, although the 2σ errors for all of the analyses are large, the final age is considered a reasonable estimate of the time of crystallization of this sample of the Mosquito Hill porphyry.

Sample HX10-53_99.7 m yielded 29 equant zircon grains and grain fragments ranging up to 200 µm in longest dimension and generally, the grains were clear to very pale yellow and ranged from euhedral, needle like to equidimensional grains. Most zircons exhibit distinctive growth zonation and locally possible inheritance (Figure 7A). Two data points were rejected because these were characterized by probabilities of concordance of <50% (Table 1). The concordia plot for all zircons also indicates potential inheritance (Figure 7B), although a group of eighteen analyses cluster together on concordia. Eight significantly older concordant

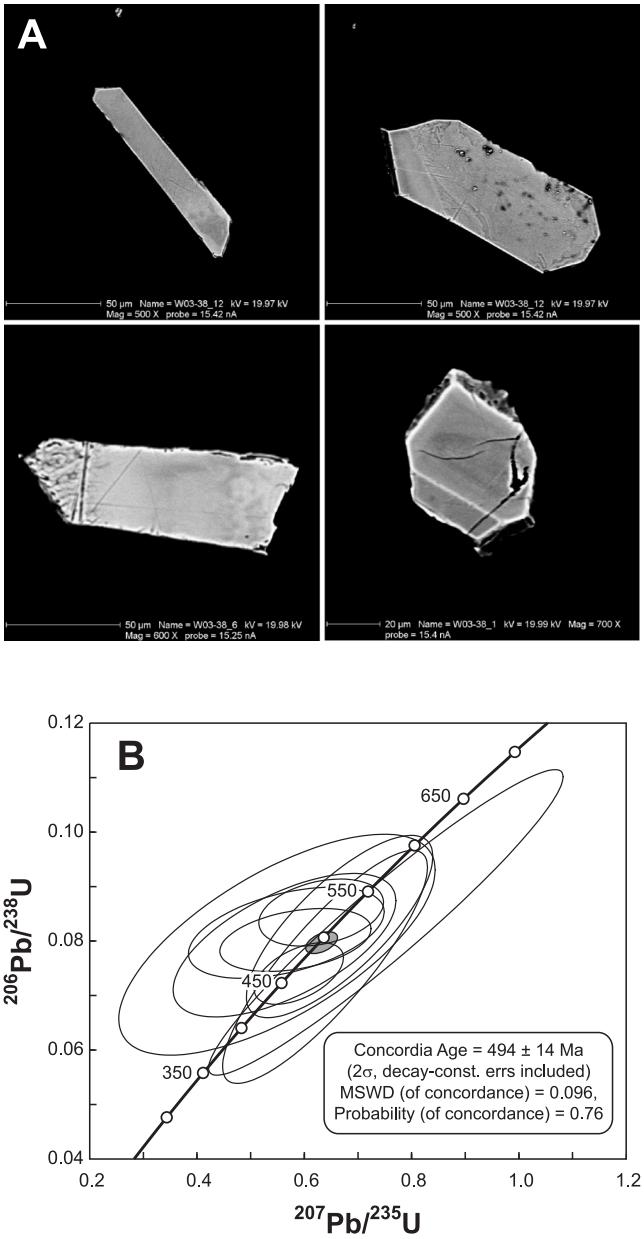

Figure 6. *A) BSE-SEM images of representative zircons from Mosquito Hill porphyry sample WO3-38. B) The U-Pb concordia diagram of all zircon analyses from sample WO3-38. Shaded ellipse represents final quoted age at 2σ.*

grains are interpreted to reflect inheritance and, when these are removed from the dataset, the remaining zircon grains define a reasonably well-fit, lower concordia intercept age of 477 ± 8 Ma (Figure 7C), overlapping, within error, the determination for the other sample of Mosquito Hill porphyry (WO3-38). The older inherited zircons yielded ages of 531, 533, 574, 915 Ma, 997, 1062, 1342 and 1774 Ma, indicating inheritance from sources as old as the Paleoproterozoic.

Table 1: U–Pb LAM-ICP-MS data

Analysis	file name	Measured Isotopic Ratios $^{207}Pb/^{235}U$	1σ error	$^{206}Pb/^{238}U$	1σ error	Rho	$^{207}Pb/^{206}Pb$	1σ error	Calculated Ages $^{207}Pb/^{235}U$ Ma	1σ error Ma	$^{206}Pb/^{238}U$ Ma	1σ error Ma
W03-38: Mosquito Hill porphyry (603792E, 5367246N zone 21 NAD27)												
1	fe20a12 1	0.63759	0.07745	0.07535	0.00881	0.85651	0.05905	0.00416	500.8	48.0	468.3	52.8
2	fe20a05 1	0.54988	0.05062	0.07590	0.00342	0.63111	0.05116	0.00284	444.9	33.2	471.6	20.5
3	fe20a06 1	0.56930	0.08804	0.07953	0.00552	0.62742	0.05079	0.00438	457.6	57.0	493.3	33.0
4	fe20a07 1	0.59347	0.05769	0.06678	0.00416	0.79326	0.06264	0.00300	473.1	36.8	416.7	25.2
5	fe20a08 1	0.50556	0.07528	0.07973	0.00249	0.29163	0.04637	0.00476	415.5	50.8	494.5	14.9
6	fe20a09 1	0.58618	0.05873	0.08023	0.00237	0.35287	0.05196	0.00407	468.4	37.6	497.5	14.1
7	fe20a13 1	0.45865	0.10302	0.07548	0.00462	0.43717	0.04519	0.00569	383.3	71.7	469.1	27.7
8	fe20a15 1	0.99751	0.10473	0.07932	0.00494	0.60705	0.08906	0.00727	702.5	53.2	492.1	29.5
9	fe20a16 1	0.57043	0.04379	0.07978	0.00236	0.52507	0.05107	0.00244	458.3	28.3	494.8	14.1
10	fe20a17 1	0.51727	0.05288	0.07607	0.00273	0.41372	0.04848	0.00384	423.3	35.4	472.6	16.4
11	fe20a24 1	0.58941	0.03395	0.07401	0.00230	0.51325	0.05490	0.00285	470.5	21.7	460.3	13.8
12	fe20a25 1	0.76088	0.13922	0.08360	0.01153	0.95376	0.06417	0.00279	574.5	80.3	517.5	68.6
13	fe20a26 1	1.60534	0.29362	0.09512	0.01150	0.51507	0.11723	0.02359	972.3	114.4	585.7	67.7
14	fe20a27 1	0.63491	0.04823	0.08526	0.00251	0.30993	0.05146	0.00465	499.1	30.0	527.4	14.9
15	fe20a28 1	0.87409	0.04462	0.09576	0.00264	0.41081	0.06133	0.00375	637.8	24.2	589.5	15.5
W12-003 (HX10-53_99.7m): Mosquito Hill porphyry (603792E, 5367246N zone 21 NAD27)												
1	se21a09	0.55470	0.09183	0.07222	0.00641	0.26808	0.05965	0.00213	448.1	60.0	449.5	38.5
2	se21a19	0.56663	0.04552	0.07321	0.00345	0.29369	0.05693	0.00101	455.8	29.5	455.4	20.8
3	se21a41	0.58897	0.04574	0.07482	0.00247	0.21251	0.06109	0.00113	470.2	29.2	465.1	14.8
4	se21a16	0.59632	0.04819	0.07465	0.00286	0.23689	0.05966	0.00139	474.9	30.7	464.1	17.1
5	se21a39	0.61470	0.05592	0.07449	0.00301	0.22244	0.06708	0.00187	486.5	35.2	463.2	18.1
6	se21a11	0.59450	0.05560	0.07529	0.00363	0.25763	0.06327	0.00164	473.7	35.4	468.0	21.7
7	se21a17	0.61527	0.04954	0.07568	0.00268	0.21975	0.06282	0.00148	486.9	31.1	470.3	16.0
8	se21a18	0.59548	0.07252	0.07612	0.00382	0.20617	0.06839	0.00260	474.4	46.2	472.9	22.9
9	se21a21	0.60251	0.03710	0.07614	0.00212	0.22568	0.06020	0.00144	478.8	23.5	473.1	12.7
10	se21a06	0.60402	0.03993	0.07609	0.00258	0.25693	0.05784	0.00109	479.8	25.3	472.7	15.5
11	se21a20	0.60167	0.03623	0.07662	0.00233	0.25263	0.05650	0.00147	478.3	23.0	475.9	14.0
12	se21a24	0.59446	0.03463	0.07697	0.00221	0.24653	0.06079	0.00124	473.7	22.1	478.0	13.2
13	se21a22	0.60856	0.07152	0.07722	0.00383	0.21129	0.05994	0.00155	482.7	45.1	479.5	22.9
14	se21a08	0.60350	0.06658	0.07775	0.00366	0.21318	0.06417	0.00176	479.5	42.2	482.7	21.9
15	se21a23	0.61893	0.07140	0.07761	0.00366	0.20452	0.05767	0.00186	489.2	44.8	481.8	21.9
16	se21a29	0.61482	0.05017	0.07836	0.00298	0.23302	0.06223	0.00155	486.6	31.5	486.3	17.8
17	se21a36	0.61721	0.04451	0.07862	0.00282	0.24861	0.06028	0.00171	488.1	27.9	487.9	16.8
18	se21a40	0.63996	0.01588	0.07659	0.00168	0.44207	0.05619	0.00057	502.3	9.8	475.7	10.1
19	se21a27	0.68138	0.06905	0.08080	0.00337	0.20603	0.06974	0.00263	527.6	41.7	500.9	20.1
20	se21a42	0.65997	0.05639	0.08301	0.00393	0.27709	0.06018	0.00128	514.6	34.5	514.1	23.4
21	se21a32	0.66450	0.06883	0.08301	0.00489	0.28456	0.06076	0.00139	517.4	42.0	514.1	29.1
22	se21a10	0.69176	0.06948	0.08554	0.00590	0.34318	0.05819	0.00138	533.9	41.7	529.1	35.0
23	se21a28	0.73285	0.08287	0.08271	0.00757	0.40447	0.05802	0.00176	558.2	48.6	512.3	45.0
24	se21a12	0.68525	0.03605	0.08654	0.00279	0.30588	0.05844	0.00083	529.9	21.7	535.0	16.5
25	se21a38	0.76842	0.06075	0.09298	0.00304	0.20685	0.06401	0.00163	578.9	34.9	573.1	17.9
26	se21a13	1.51101	0.11443	0.15084	0.00656	0.28702	0.07572	0.00130	934.8	46.3	905.7	36.7
27	se21a33	1.68048	0.09683	0.16688	0.00569	0.29592	0.07317	0.00173	1001.2	36.7	994.9	31.4
28	se21a30	1.81791	0.16549	0.17990	0.00812	0.24799	0.07801	0.00182	1051.9	59.6	1066.4	44.4
29	se21a37	2.75174	0.13479	0.23136	0.00590	0.26017	0.08854	0.00166	1342.6	36.5	1341.6	30.9
30	se21a31	4.82701	0.94118	0.31092	0.04189	0.34550	0.11483	0.00190	1789.6	164.0	1745.2	206.0
W12-003 (HX10-53_212.7m): dacitic dyke (603792E, 5367246N zone 21 NAD27)												
1	se19a47	0.53590	0.03520	0.07018	0.00231	0.25084	0.05738	0.00118	435.7	23.3	437.3	13.9
2	se19a32	0.54784	0.04852	0.07116	0.00246	0.19504	0.06233	0.00148	443.6	31.8	443.2	14.8
3	se19a35	0.56153	0.03725	0.07195	0.00245	0.25665	0.05962	0.00126	452.5	24.2	447.9	14.7
4	se19a46	0.56404	0.04298	0.07267	0.00235	0.21250	0.06085	0.00119	454.2	27.9	452.2	14.1
5	se19a54	0.55920	0.03702	0.07284	0.00275	0.28494	0.05833	0.00128	451.0	24.1	453.2	16.5
6	se19a53	0.57665	0.09239	0.07277	0.00576	0.24713	0.06595	0.00156	462.3	59.5	452.8	34.6
7	se19a43	0.56856	0.02624	0.07305	0.00230	0.34145	0.05380	0.00087	457.1	17.0	454.5	13.8
8	se19a42	0.57970	0.04532	0.07301	0.00270	0.23617	0.05767	0.00108	464.3	29.1	454.2	16.2
9	se19a51	0.57752	0.02702	0.07348	0.00174	0.25259	0.05422	0.00107	462.9	17.4	457.1	10.4
10	se19a56	0.56891	0.11875	0.07395	0.00445	0.14400	0.06735	0.00188	457.3	76.9	459.9	26.7
11	se19a34	0.58422	0.06203	0.07469	0.00369	0.23280	0.05897	0.00115	467.2	39.8	464.4	22.2
12	se19a45	0.58998	0.02970	0.07514	0.00152	0.20128	0.05617	0.00129	470.9	19.0	467.0	9.1
13	se19a38	0.60011	0.03728	0.07637	0.00189	0.19923	0.05386	0.00181	477.3	23.7	474.4	11.3
14	se19a41	0.61087	0.04947	0.07770	0.00309	0.24547	0.05933	0.00148	484.1	31.2	482.4	18.5
15	se19a36	0.61182	0.03307	0.07812	0.00244	0.28878	0.05219	0.00117	484.7	20.8	484.9	14.6
16	se19a44	0.61258	0.10187	0.07816	0.00682	0.26244	0.05471	0.00149	485.2	64.1	485.1	40.8
17	se19a31	0.67793	0.10308	0.08125	0.00543	0.21959	0.06306	0.00160	525.5	62.4	503.6	32.3
18	se19a55	0.65190	0.03905	0.08184	0.00253	0.25763	0.06041	0.00125	509.7	24.0	507.1	15.1
19	se19a52	0.67082	0.06825	0.08396	0.00539	0.31553	0.05882	0.00191	521.2	41.5	519.7	32.1
20	se19a33	0.71362	0.06913	0.08866	0.00410	0.23890	0.06273	0.00126	546.9	41.0	547.6	24.3
21	se19a48	0.73817	0.04095	0.09047	0.00256	0.25484	0.05958	0.00125	561.3	23.9	558.3	15.1
22	se19a37	5.19882	0.24030	0.31521	0.01087	0.37288	0.11199	0.00113	1852.4	39.4	1766.3	53.3

Table 2: ^{40}Ar–^{39}Ar thermochronological data. Plateau segments marked with an asterisk

Lab #: D-673e:
Sample: HX06-16-130.9 sericite
J Value: 0.016907 ± 0.000038

Power	$^{36}Ar/^{40}Ar$	±	$^{39}Ar/^{40}Ar$	±	r	Ca/K	$\%^{40}Atm$	$^{40}Ar^*/^{39}K$	±	$\%^{39}Ar$	Age	±
1.80	0.000711	0.000080	0.078876	0.000854	0.004	0.040	20.94	10.02	0.32	1.10	282.2	8.3
2.00	0.000176	0.000054	0.064227	0.000670	0.001	0.082	5.20	14.76	0.30	1.07	401.9	7.2
2.30	0.000071	0.000021	0.064017	0.000407	0.001	0.540	2.09	15.29	0.14	2.98	414.9	3.4
2.50	0.000030	0.000015	0.064677	0.000390	0.001	0.371	0.89	15.32	0.12	4.20	415.6	2.8
2.70	0.000032	0.000013	0.065063	0.000415	0.001	0.301	0.96	15.22	0.12	5.07	413.2	2.8
2.90	0.000029	0.000021	0.065627	0.000402	0.000	0.241	0.84	15.11	0.13	5.99	410.4	3.3
3.10	0.000027	0.000018	0.065773	0.000417	0.001	0.140	0.79	15.08	0.13	6.24	409.8	3.1
3.30	0.000021	0.000015	0.065929	0.000401	0.001	0.173	0.62	15.07	0.11	6.37	409.6	2.8
3.50	0.000027	0.000014	0.066070	0.000441	0.001	0.200	0.79	15.01	0.12	6.36	408.1	2.9
3.70	0.000023	0.000017	0.066221	0.000426	0.001	0.259	0.68	15.00	0.12	8.47	407.7	3.0
3.8*	0.000026	0.000016	0.066364	0.000426	0.001	0.184	0.77	14.95	0.12	6.54	406.6	2.9
3.9*	0.000026	0.000015	0.066443	0.000367	0.001	0.171	0.77	14.93	0.11	5.32	406.2	2.6
4.00*	0.000036	0.000018	0.066387	0.000339	0.001	0.165	1.06	14.90	0.11	4.37	405.4	2.8
4.10*	0.000028	0.000020	0.066380	0.000425	0.000	0.194	0.84	14.94	0.13	4.18	406.3	3.2
4.20*	0.000030	0.000015	0.066344	0.000371	0.000	0.123	0.89	14.94	0.11	3.81	406.3	2.6
4.40*	0.000026	0.000015	0.066492	0.000434	0.001	0.085	0.77	14.92	0.12	4.85	405.9	2.9
4.60*	0.000031	0.000017	0.066513	0.000435	0.000	0.088	0.92	14.90	0.12	5.03	405.2	3.0
4.80*	0.000035	0.000015	0.066643	0.000450	0.001	0.082	1.05	14.85	0.12	5.12	404.1	3.0
5.00*	0.000032	0.000018	0.066500	0.000449	0.000	0.091	0.96	14.89	0.13	3.82	405.2	3.2
5.50*	0.000027	0.000017	0.066842	0.000456	0.000	0.075	0.78	14.84	0.13	4.97	404.0	3.1
6.00*	0.000030	0.000017	0.067297	0.000383	0.001	0.091	0.88	14.73	0.11	4.15	401.1	2.8

Lab #: D-684
Sample: HX06-16-135.3 sericite
J Value: 0.016905 ± 0.000036

Power	$^{36}Ar/^{40}Ar$	±	$^{39}Ar/^{40}Ar$	±	r	Ca/K	$\%^{40}Atm$	$^{40}Ar^*/^{39}K$	±	$\%^{39}Ar$	Age	±
1.80	0.001191	0.000220	0.056037	0.001020	-0.005	0.020	35.12	11.57	1.18	0.85	322.2	30.2
2.10	0.000157	0.000035	0.061951	0.000437	0.002	0.129	4.64	15.39	0.20	6.13	417.2	4.8
2.40*	0.000033	0.000021	0.065922	0.000455	0.001	0.191	0.96	15.02	0.14	10.84	408.3	3.4
2.70*	0.000024	0.000017	0.066511	0.000479	0.000	0.084	0.71	14.93	0.13	14.18	406.0	3.2
2.90*	0.000031	0.000023	0.066179	0.000432	0.000	0.035	0.90	14.97	0.14	13.29	407.1	3.5
3.10*	0.000030	0.000026	0.066400	0.000579	0.000	0.001	0.87	14.93	0.17	13.45	406.0	4.3
3.30*	0.000027	0.000022	0.066689	0.000418	0.001	0.014	0.79	14.88	0.14	10.65	404.7	3.3
3.50*	0.000020	0.000022	0.066874	0.000409	0.000	0.002	0.60	14.86	0.14	8.67	404.4	3.3
3.70*	0.000020	0.000029	0.066919	0.000405	0.000	0.013	0.58	14.86	0.16	5.89	404.2	3.8
4.00*	0.000022	0.000026	0.066915	0.000439	0.000	0.003	0.66	14.85	0.15	5.34	404.0	3.7
4.30*	0.000037	0.000035	0.066350	0.000574	0.000	0.025	1.10	14.91	0.20	4.10	405.4	4.9
4.60*	0.000035	0.000044	0.066148	0.000613	0.000	0.006	1.04	14.96	0.24	2.84	406.8	5.9
5.00	0.000087	0.000069	0.066208	0.000846	0.000	0.014	2.56	14.72	0.36	1.79	400.8	8.8
6.00	0.000306	0.000061	0.064354	0.000788	0.001	0.362	8.98	14.14	0.33	1.99	386.7	8.1

The third sample (W12-003: HX10-53_212.7 m) of a feldspar porphyritic dacitic dyke crosscutting the basal mélange immediately below mylonitized porphyry yielded 22 zircons (Figure 8A). These generally equant zircon grains and grain fragments appear very similar to those described above from samples WO3-38 and HX10-53_99.7 m. Three analyses were rejected from the age calculation including two that are slightly older than the majority and may exhibit some inheritance, and a third that is clearly an inherited grain and yielded a discordant, Paleoproterozoic date of 1827 Ma (Table 1 and Figure 8B). The remaining nineteen analyses yielded a fairly tight cluster of data on, or near, concordia and yielded a concordia age of 464 ± 7 Ma, interpreted to represent the age of the crosscutting dyke (Figure 8C).

^{40}Ar–^{39}Ar RESULTS

The ^{40}Ar–^{39}Ar laser step-heating ages were determined for grain separates of coarse (250 to 350 μm), randomly oriented sericite grains extracted from two samples of sericite-carbonate-altered and mineralized Mosquito Hill porphyry (samples HX06-16_130.9 m and HX06-16_ 135.3 m). The ^{40}Ar–^{39}Ar data are given in Table 2.

Sericite from HX06-16_130.9 m yielded a mildly disturbed argon release spectrum characterized by a series of gently decreasing gas release steps (Figure 9A). Eleven of the high temperature steps, representing 56.5% of the total ^{39}Ar released, yielded a plateau age of 405.8 ± 1.3 Ma (MSWD=0.53, POP= 0.87). Although this analysis does not

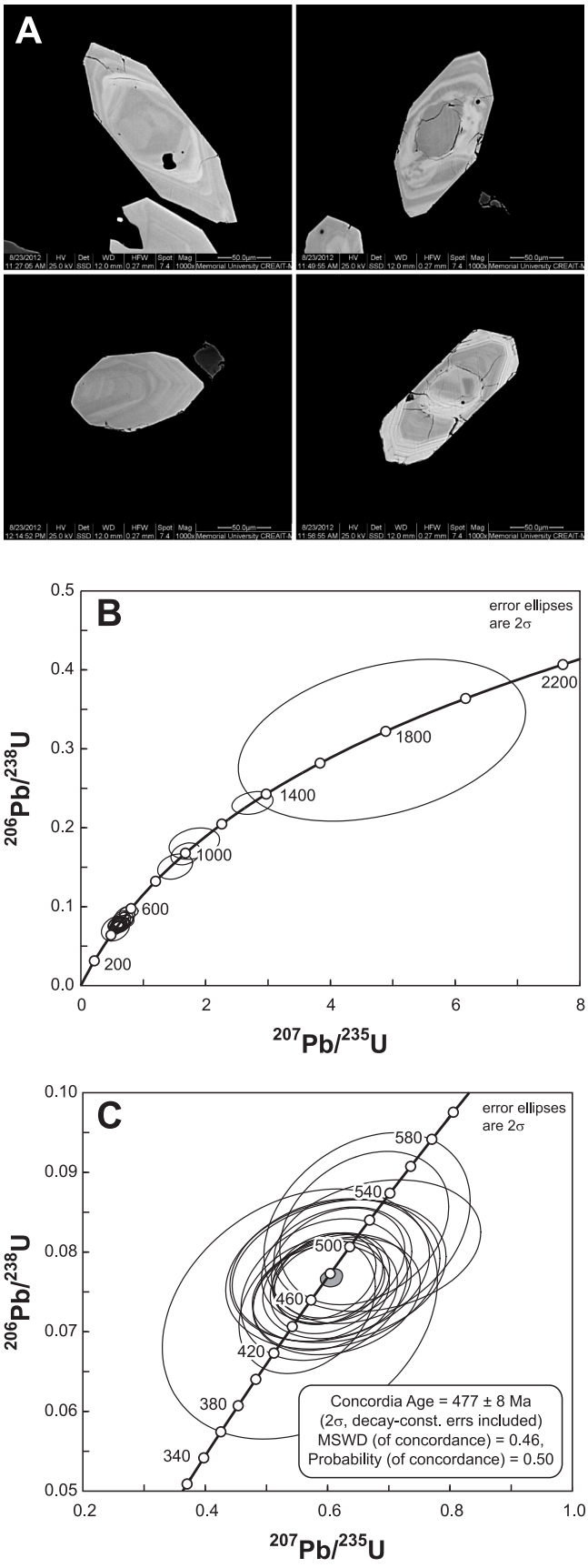

Figure 7. (opposite) *A) BSE-SEM images of representative zircons from Mosquito Hill porphyry sample HX10-53_99.7m. B) U–Pb concordia diagram of all zircon data from sample HX10-53_99.7 m. C) U–Pb concordia diagram of best-fit, igneous zircon data from sample HX10-53_99.7 m. Shaded ellipse represents final quoted age at 2σ.*

conform to the strict criteria for a plateau age, as it contained only 56.5% of the ^{39}Ar released, it is identical, within error, to that of HX06-16_135.3 m and defines a series of ten ^{40}Ar–^{39}Ar age steps with reasonably low excess scatter. This age is, therefore, interpreted to represent the age of the hydrothermal event responsible for deposition of the mica.

A sericite concentrate from HX06-16_135.3 m yielded a well-defined argon release spectrum characterized by a flat segment consisting of 10 of 14 gas release steps (Figure 9B: 89.2% of the total ^{39}Ar released) that overlap within error. These steps yielded a plateau age of 405.7 ± 1.4 Ma (MSWD=0.63, POP= 0.78), that is inferred to represent the time of formation of the sericite and hence the age of the hydrothermal event and fluids responsible for deposition of the mica.

IMPLICATIONS OF NEW FIELD, PETROGRAPHIC AND GEOCHRONOLOGICAL DATA

The setting of the Mosquito Hill gold deposit is particularly important as it occurs along the contact zone between the ophiolitic rocks of the Coy Pond Complex and, the felsic volcanic, volcaniclastic and sedimentary rocks of the North Steady Pond Formation of the Cambro-Ordovician Baie D'Espoir Group (Colman-Sadd, 1985; Colman-Sadd *et al*., 1992; Sandeman *et al.*, 2012).

Mineralization at Mosquito Hill comprises disseminated euhedral arsenopyrite and subhedral pyrite in the matrix of a sericite-Fe carbonate-altered quartz-plagioclase ± biotite ± hornblende-bearing subvolcanic dacite intrusion and associated volcaniclastic tuffs. Although anomalous gold assays have been obtained from the adjacent tuffs, volcaniclastic rocks and mélange, these values are relatively low and are not considered economic. Free gold has not been observed, but higher concentrations of gold is directly correlated with abundant euhedral arsenopyrite, suggesting that the gold may, in fact, be incorporated in the crystal lattice of the arsenopyrite. This will be tested *via* LAM-ICP-MS trace-element analysis of sulphide minerals from the deposit.

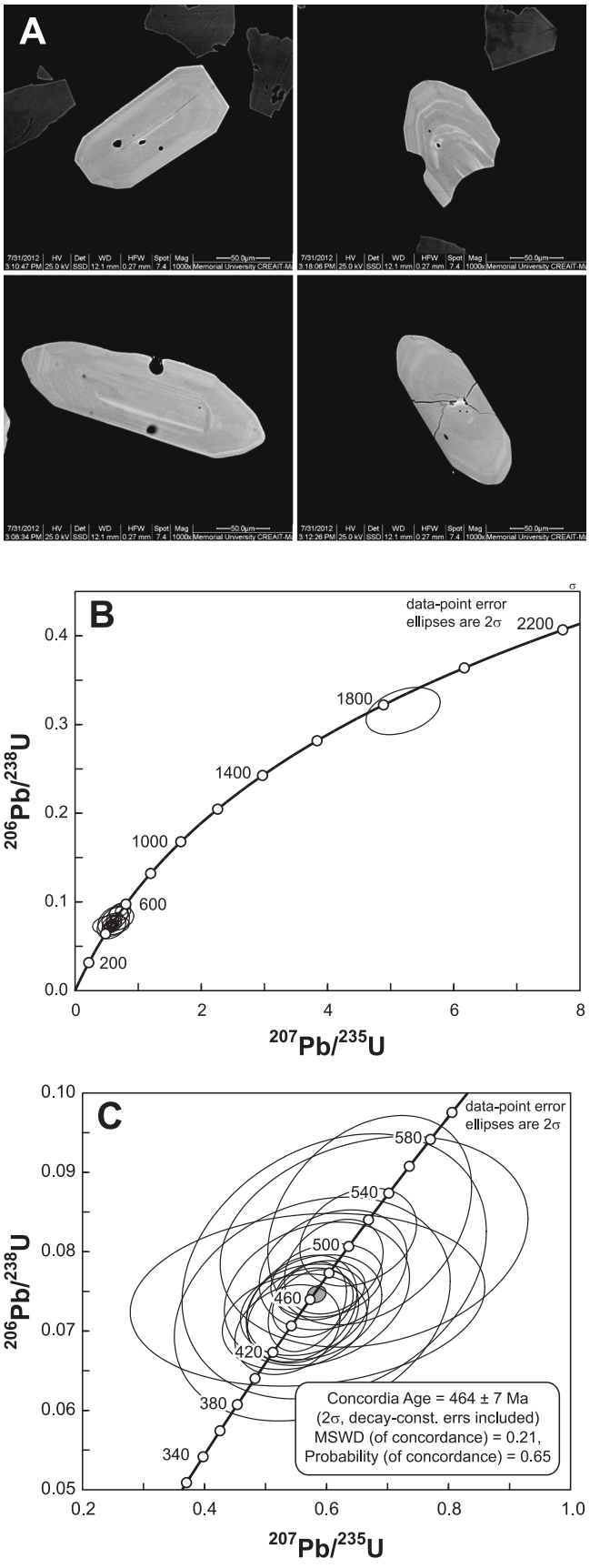

Figure 8. (opposite) *A) BSE-SEM images of representative zircons from dacitic dyke HX10-53_212.7 m. B) U–Pb concordia diagram of all zircon data from sample HX10-53_212.7 m. C) U–Pb concordia diagram of best-fit, igneous zircon data from sample HX10-53_212.7 m. Shaded ellipse represents final quoted age at 2σ.*

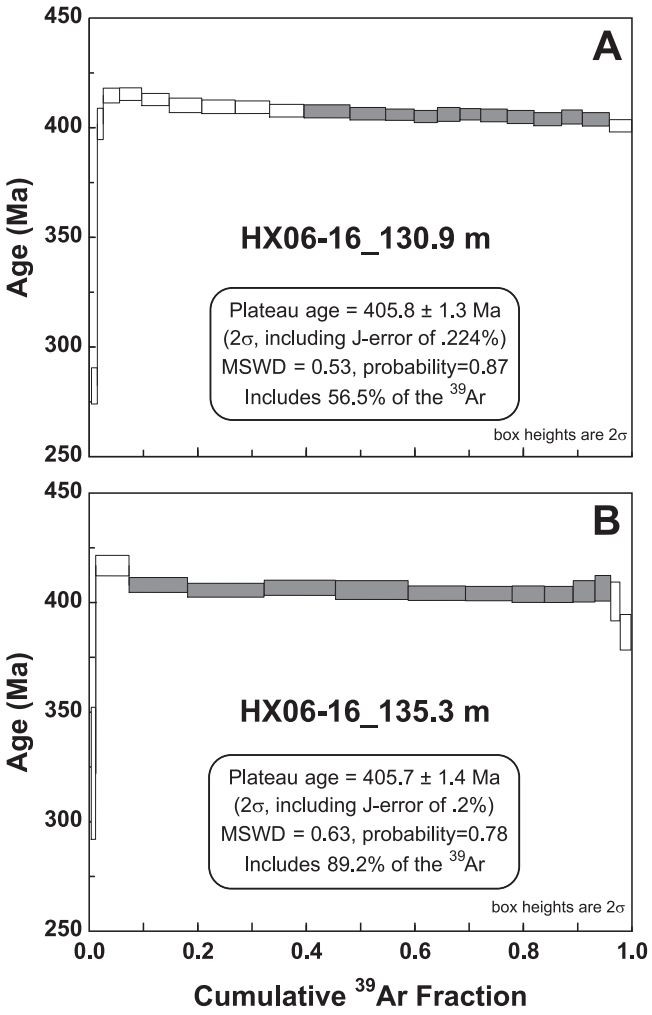

Figure 9. *The ^{40}Ar–^{39}Ar gas release spectra for 2 samples of coarse-grained (<350 to >250 μm), randomly oriented sericite separated from mineralized Mosquito Hill porphyry from drillhole HX06-16. Plateau segments shown as shaded boxes.*

Historical U–Pb geochronology on the crystallization ages and high-*T* metamorphism of some of the igneous rocks in the region provide only broad constraints on the tectonomagmatic history and, in particular, emphasize their Ordovician magmatic, sedimentological and tectonic history. Available geochronological data for the region are presented in Figure 10 and are supplemented with the data presented herein. The new U–Pb and ^{40}Ar–^{39}Ar geochronological data along with stratigraphical and structural data for the Mosquito Hill porphyry and volcaniclastic sandstones establish that mineralized porphyritic dacite crystallized in the Late Cambrian to Early Ordovician at 494 ± 14 and 477 ± 8 Ma. The unmineralized porphyritic dacitic dyke that crosscuts a portion of the mélange immediately below mylonitized MHP yielded an age of 464 ± 7 Ma, indicating that, at least, some of the mélange, structurally below the Mosquito Hill mineralization, was formed prior to 464 Ma.

Randomly oriented, posttectonic, but apparently synmineralization sericite in the Mosquito Hill porphyry, yield precise, reproducible ^{40}Ar–^{39}Ar plateau cooling ages of 406 Ma. These cooling ages are much younger than the Cambro-Ordovician crystallization ages for the rocks, but are comparable to and overlapping, within error, with late Early Devonian granitoids in the Meelpaeg Subzone to the west (Dunning *et al.,* 1990; van Staal *et al.,* 2005) and young phases of the Mount Peyton Batholith to the immediate northeast (O'Driscoll, 2006; McNicoll *et al.,* 2006; Dickson *et al.,* 2007).

The Late Cambrian to Ordovician ages obtained for the two samples of mineralized porphyry overlap, within error, but their mean ages are significantly different. As the samples were obtained from widely spaced and differing stratigraphic levels, the possibility remains that these two porphyry samples may represent distinct intrusions (*i.e*., there is more than one porphyry). Similarly, the younger MHP zircon age (477 ± 8 Ma) overlaps, within error, the age for the crosscutting dyke (464 ± 7 Ma) and, the more precise, thermal ionization mass spectrometric (TIMS) age of 468 ± 2 Ma determined for a felsic volcanic rock of the Twillick Brook Member, lying ~30 km to the south-southeast of Mosquito Hill (Colman-Sadd *et al*., 1992). These new LAM-ICP-MS zircon ages provide only broad time constraints on the age range of the felsic volcanic rocks of the region. Greater analytical precision is required to confidently determine if these felsic volcanic units are distinct in age. More precise geochronological data might be obtained through either follow up TIMS or SHRIMP U–Pb geochronology of the zircon grains.

Broadly time-equivalent correlatives of the Mosquito Hill porphyry and North Steady Pond Formation volcaniclastic rocks exposed in the Exploits Subzone are common farther west and include the *ca*. 495 Ma Tulks Hill belt (Evans *et al.*, 1990; Zagorevski *et al.*, 2007; Hinchey, 2011) and the *ca*. 465 Ma Red Cross Group (Valverde-Vaquero *et al.*, 2006), respectively. Although of similar age, these western Exploits Subzone volcanic sequences contain significant quantities of both felsic and mafic volcanic rocks, whereas the North Steady Pond Formation in the eastern Exploits Subzone contains dominantly intermediate to felsic volcanic rocks that are accompanied by widespread, quartzose volcaniclastic and siliciclastic sedimentary units. On the basis of facies, therefore, the sequences of the eastern Exploits Subzone appear to differ significantly from those of the western Exploits Subzone.

Field relationships determined from trenches as well as in diamond-drill holes at Mosquito Hill indicate that the bounding surfaces between the Coy Pond Complex and the Baie D'Espoir Group dip moderately (~50°) to the south and southeast and are defined by a mélange unit containing ultramafic, siliciclastic sedimentary and sericite–pyrite–arsenopyrite-altered quartz-porphyry clasts (House, 2006; House and Newport, 2007; *this study*). A portion of the mélange is crosscut by a 464 ± 7 Ma intermediate dyke indicating that some of the mélange must have formed prior to that time in the Ordovician. The origin of the sericite-altered porphyry clasts in the mélange is not presently known, however, ongoing petrological studies of the clasts will help to determine if they represent Mosquito Hill porphyry or alternatively porphyritic trondhjemite derived from the adjacent Reid gold deposit (formed at 510 ± 4 Ma: Sandeman *et al.*, 2012) or some other 'exotic' source.

The Coy Pond Complex–Baie D'Espoir Group contact zone is, therefore, more structurally complex than previously recognized, and the possibility exists that the contact zone preserves a number of discrete, deformation zones (imbricate thrust zones). These were focused within intervals of tectonic mélange containing black shale, polymict conglomerate, serpentinized peridotite and altered quartz-feldspar porphyry clasts. An understanding of the mélange interval is critical to an enhanced understanding of the tectonic history of the area, the cause of hydrothermal fluid flow in the region and the accompanying deposition of gold. If the altered porphyry clasts represent altered, eroded Reid deposit trondhjemite (Sandeman *et al*., 2012) then, as we do not yet know the age of gold mineralization at the Reid deposit, the mélange may have formed in association with thrust nappe assembly and uplift and erosion of Penobscot arc rocks during the Ordovician. However, if the altered porphyry clasts represent Mosquito Hill porphyry, then portions of the mélange must represent a unit deposited, at least in part, after *ca*. 406 Ma, the minimum age of the sericite alteration. If the latter hypothesis is true, an Ordovician mélange has been re-utilized during the Late Silurian–Early Devon-

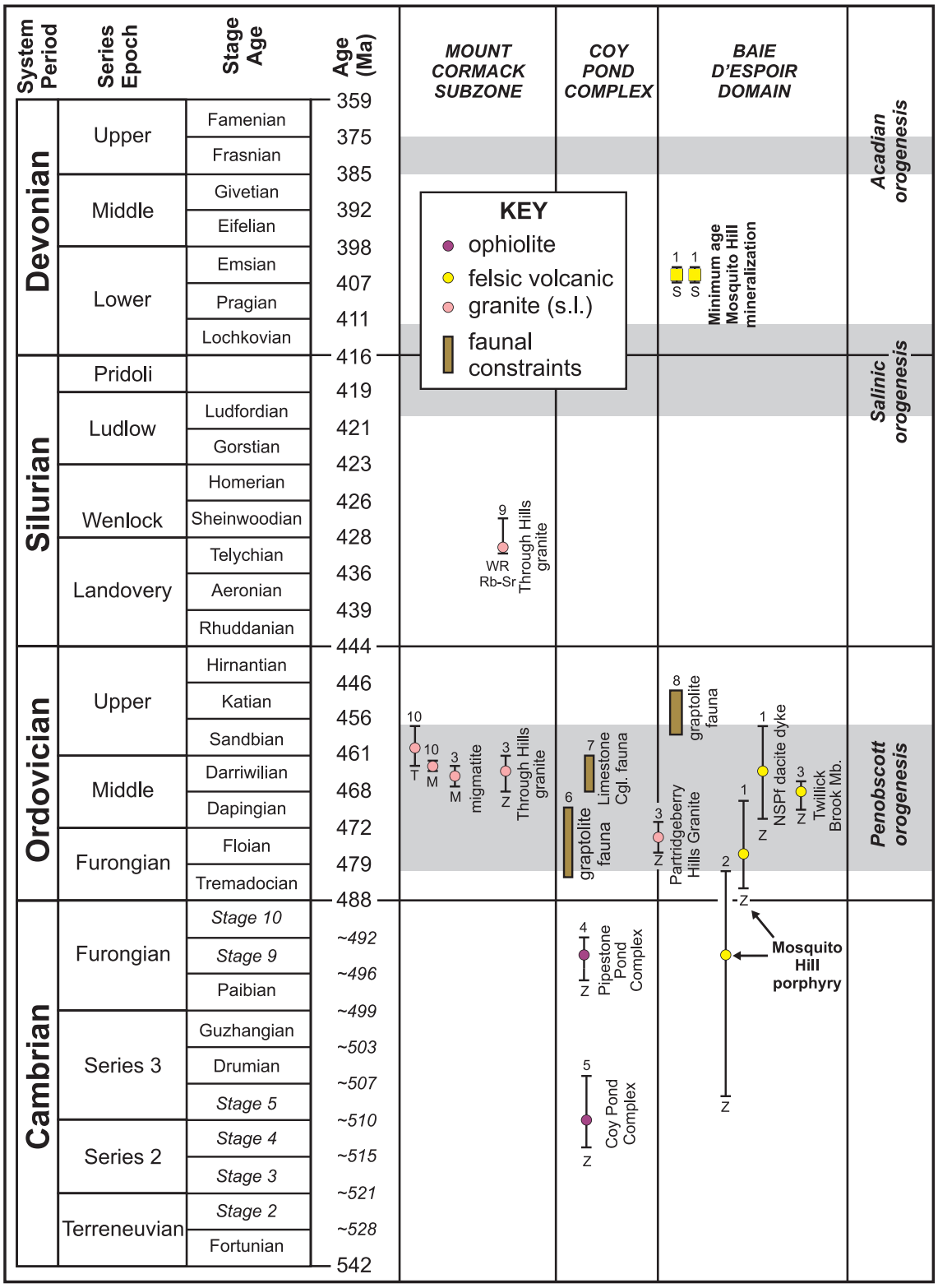

Figure 10. *Summary of geochronological data for the region subdivided by geography and tectonostratigraphic zone. Data sources: 1) This study; 2) O'Driscoll (2006); 3) Colman-Sadd* et al. *(1992); 4) Dunning and Krogh (1985); 5) Sandeman* et al. *(2012); 6) Williams* et al. *(1992); 7) Dec and Colman-Sadd (1990); 8) Williams (1991); 9) Elias and Strong (1982); 10) Valverde-Vaquero* et al. *(2006). The letter below each age represents the mineral analyzed. S – sericite; Z – zircon; M – monazite; T – titanite; Rb–Sr WR – whole-rock, rubidium-strontium isochron.*

ian, likely in advance of northwestward-propagating thrust sheets. This hypothesis may be tested through lithogeochemical and isotopic analysis of the altered porphyry clasts. Similarly, ^{40}Ar–^{39}Ar thermochronology on sericite deposited with arsenopyrite and gold in the adjacent Reid gold deposit would constrain the age of that mineralization and assist in determining the source of the altered quartz-feldspar porphyry clasts in the mélange. The Sm–Nd analyses of the two distinct porphyry intrusions and the altered porphyry clasts will aid in the petrological interpretations of these rocks and may further refine the antiquity of their magmatic sources and assist in new tectonic interpretations of the eastern Exploits Subzone.

ACKNOWLEDGMENTS

The ^{40}Ar–^{39}Ar samples were analyzed by Dr. D. Archibald of Queen's University. Matthew Minnett and Jonathon Hull provided capable assistance in the field while Gerry Hickey helped immensely with logistics and safety. An earlier version of the manuscript was improved by the helpful reviews of Bruce Ryan, and this version by the reviews of Andy Kerr. Golden Dory Resources Corporation and Paragon Minerals Corporation (now Canadian Zinc Corp.) are kindly thanked for permission to study the Mosquito Hill deposit and for unlimited access to data. This research has been partially funded through a Research and Development Corporation of Newfoundland and Labrador (RDC) GeoExplore 2010-2013 Research Grant to James Conliffe and Derek Wilton.

REFERENCES

Blackwood, R.F.
1982: Geology of the Gander Lake (2D/15) and Gander River (2D/2) area: Newfoundland Department of Mines and Energy, Mineral Development Division, Report 82-4, 56 pages.

Colman-Sadd, S.P.
1980: Geology of south–central Newfoundland and evolution of the eastern margin of Iapetus. American Journal of Science, Volume 280, pages 991-1017.

1982: West Gander Rivers (2D/11), west portion, Newfoundland. Newfoundland Department of Mines and Energy, Mineral Development Division, Open File Map 82-59.

1985: Geology of the Burnt Hill map area (NTS 2D/5), Newfoundland. Newfoundland Department of Mines and Energy, Mineral Development Division, Report 85-3, 108 pages includes map 85-001 Burnt Hill, scale 1:50 000.

Colman-Sadd, S.P., and Russell, H.A.J.
1988: Miguels Lake (2D/12), Newfoundland. Newfoundland Dpartment of Mines and Energy, Mineral Development Division, Map 88-50.

Colman-Sadd, S.P. and Swinden, H.S.
1982: Geology and mineral potential of south-central Newfoundland. Newfoundland Department of Mines and Energy, Mineral Development Division, Report 82-8, 102 pages.

1984: A tectonic window in central Newfoundland? Geological evidence that the Appalachian Dunnage Zone may be allochthonous. Canadian Journal of Earth Sciences, Volume 21, pages 1349-1367.

Colman-Sadd, S.P., Dunning, G.R. and Dec, T.
1992: Dunnage–Gander relationships and Ordovician orogeny in central Newfoundland: A sediment provenance and U/Pb age study. American Journal of Science, Volume 292, pages 317-355.

Davenport, P.H., Nolan, L.W. and Honarvar, P.
1994: Geochemical Atlas of the Island of Newfoundland. Newfoundland Department of Mines and Energy, Geological Survey Branch, Open File NFLD/2355, scale 1:1 000 000.

Dec, T. and Colman-Sadd, S.P.
1990: Timing of ophiolite emplacement onto the Gander Zone: evidence from providence studies in the Mount Cormack Subzone. *In* Current Research. Newfoundland Department of Mines and Energy, Geological Survey Branch, Report 90-1, pages 289-303.

Dickson, W.L., McNicoll, V.J., Nowlan, G.S. and Dunning, G.R.
2007: The Indian Islands Group and its relationships to adjacent units: recent data. *In* Current Research. Newfoundland Department of Natural Resources, Geological Survey, Report 07-1, pages 1-9.

Dimmell, P.
2004: First and second year (2004) assessment report (Geochemistry (lake bottom), induced polarization, geological mapping and prospecting, petrology, diamond drilling, environmental baseline studies) on the Reid option property Datan Resources Inc. First-year licence 9697M second year licences 9073M, 9080M, 9081M, 9082M, 9096M, 9138M, 9139M, 9302M, 9308M, 9344M, 9345M, 9347M and 9348M. Northwest Gander River area, Central NF. NTS 2/D5 2D12. NFLD/002D/0574.

Dimmell, P.M., Scott, W.J. and Woods, D.V.
2003: First year assessment report on prospecting and geochemical, geophysical, trenching and diamond drilling exploration for licences 9073M, 9080M-9082M and 9096M on claims in the Northwest Gander River area, central Newfoundland, NTS 2/D5. NFLD/002D0515.

Dunning, G. R. and Krogh, T. E.
1985. Geochronology of ophiolites of the Newfoundland Appalachians. Canadian Journal of Earth Sciences, Volume 22, pages 1659-1670.

Dunning, G.R., O'Brien, S.J., Colman-Sadd, S.P., Blackwood, R.F., Dickson, W.L., O'Neill, P.P. and Krogh, T.E.
1990: Silurian Orogeny in the Newfoundland Appalachians. Journal of Geology, Volume 98, pages 895–913.

Elias, P. and Strong, D.F.
1982: Paleozoic granitoid plutonism of southern Newfoundland: contrasts in timing, tectonic setting and level of emplacement. Transactions of the Royal Society of Edinburgh, Volume 73, pages 43-57.

Evans, D.
2010: 12th year assessment report exploration work Mosquito Hill Zone, Huxter Lane Property Licence 016636M NTS 2D/05, Northwest Gander River area, central Newfoundland. Golden Dory Resources Corporation and Paragon Minerals Corporation, unpublished report, December 2010, 18 pages.

2011: Ninth year assessment report on diamond drilling, Reid Porphyry Zone, Brady Property Mineral Licence 018700M Newfoundland and Labrador. Golden Dory Resources Corp., unpublished report, September, 2011, 71 pages.

Evans, D.T.W., Kean, B.F. and Dunning, G.R.
1990: Geological studies, Victoria Lake Group, central Newfoundland. *In* Current Research. Newfoundland Department of Mines and Energy, Geological Survey, Report 90-1, pages 131-144.

Evans, D. and Vatcher, S.
2009: Diamond drilling program Mosquito Hill Zone, Huxter Lane Property Licences 11926M and 12835M NTS 2D/05, Northwest Gander River area, central Newfoundland. Golden Dory Resources Corporation and Paragon Minerals Corporation, unpublished report, July 2009.

Evans, D., Vatcher, S. and Dimmell, P.M.
2007: Assessment report on prospecting, rock and soil sampling Brady Property 2D/5 and 2D/12, licences 9073M, 9080M, 9081M, 9082M, 9302M, 11858M, 11859M, 12877M, 13122M, 13267M and 13268M Newfoundland and Labrador. NFLD/002D0689.

Festa, A., Dilek, Y., Pini, G.A., Codegone, G. and Ogata, K.
2012: Mechanisms and processes of stratal disruption and mixing in the development of mélanges and broken formations: redefining and classifying mélanges. Tectonophysics, Volume 568-569, pages 7-24.

Giroux, G.H. and Froude, T.
2010: FORM 43-101F1 technical report for the Mosquito Hill zone resource estimate, Huxter Lane option Grand Falls–Windsor–Buchans Electoral District NTS: 2D/5 Newfoundland and Labrador for Golden Dory Resources Corp. and Paragon Minerals Corporation. SEDAR website.

Hinchey, J.
2011: The Tulks Volcanic Belt, Victoria Lake Supergroup, central Newfoundland – geology, tectonic setting and volcanogenic massive sulphide mineralization. Newfoundland Department Natural Resources, Geological Survey, Report 11-2, 167 pages.

House, S.
2005: Assessment report - Huxter Lane Project, Licence 8816M (3rd year) Newfoundland NTS 2D/05: Report on prospecting and rock sampling, October 2005, 21 pages.

2006: Assessment report - Huxter Project, Licences 6380M (7th year), 8396M & 8397M (4th year) Newfoundland NTS 2D/05: Report on trenching, mapping, geophysical survey, prospecting and channel/rock/soil sampling, March 2006, 104 pages.

2008: Assessment report on diamond drilling, prospecting and soil sampling on Licences 11926M (9th year), 12835M (1st year), 11787M (2nd year), and 11880M (2nd year) for the Huxter Lane Property, central Newfoundland, March 2008. 27 pages.

House, S. and Newport, A.M.
2007: Assessment report on airborne geophysics and diamond drilling on Licence 11926M (8th year) for the Huxter Lane Property, central Newfoundland, NTS 2D/05, March 2007, 31 pages.

Kosler, J., Fonneland, H., Sylvester, P., Tubrett, M. and Peterson, R.
2002: U-Pb dating of detrital zircon for sediment provenance studies - a comparison of laser ablation ICPMS and SIMS techniques. Chemical Geology, Volume 182, pages 605-618.

Liverman, D. and Taylor, D.
1990: Surficial geology map of insular Newfoundland. *In* Current Research. Newfoundland Department of Natural Resources, Geological Survey, Report 90-1, pages 39-48.

Ludwig, K.R.
2003: User's manual for Isoplot/Ex rev. 3.00: a Geochronological Toolkit for Microsoft Excel. Special Publication, 4, Berkeley Geochronology Center, Berkeley, 70 pages.

MacVeigh, J.G.
2004: Assessment report on soil sampling on Licence 8816M, rock Sampling on licence 6380M, and Induced Polarization Geophysical Survey on Licences 8816M, 8397M and 6380M on the Huxter Lane Property – Licence 6380M, 6th Year, Licence 8397M, 3rd year and 8816M, 2nd year Assessment Report, Newfoundland NTS 02D/05.

McDougall, I. and Harrison, T.M.
1988: Geochronology and thermochronology by the ^{40}Ar–^{39}Ar method. Oxford Monographs on Geology and Geophysics #9, Oxford, United Kingdom, Oxford University Press, 212 pages.

McNicoll, V.J., Squires, G.C., Wardle, R.J., Dunning, G.R., and O'Brien, B.H.
2006: U-Pb geochronological evidence for Devonian deformation and gold mineralization in the eastern Dunnage Zone, Newfoundland. *In* Current Research. Newfoundland Department of Natural Resources Geological Survey, Report 06-1, pages 45-61.

Minnett, M., Sandeman, H. and Wilton, D.
2012: Geochemistry of the host rocks and timing of gold-electrum mineralization at the Viking property, Newfoundland. *In* Current Research. Newfoundland Department of Natural Resources, Geological Survey, Report 12-1, pages 61-84.

O'Driscoll, J.M.
2006: An integrated geological, geochemical, isotopic and geochronological study on the auriferous systems in the Botwood Basin and environs, central Newfoundland. Unpublished M.Sc. thesis, Memorial University of Newfoundland and Labrador, St. John's, 319 pages.

Proudfoot, D.N., Scott, S., St. Croix, L. and Taylor, D.M.
2005: Surficial geology of the Burnt Hill map sheet (NTS 2D/05). Government of Newfoundland and Labrador, Department of Natural Resources, Geological Survey. Scale 1:50 000. Map 2005-08, Open File 02D/05/0586.

Quinlan, R. and Quinlan, L.
1999: First year assessment report on prospecting, trenching and geochemical exploration for licence 6380M on claims in the Huxter Pond area, south-central Newfoundland. Newfoundland and Labrador Geological Survey, Assessment File 2D/05/0563, 1999, 27 pages.

Reynolds, P.H.
1992: Low temperature thermochronology by the ^{40}Ar–^{39}Ar method. *In* Low Temperature Thermochronology. *Edited by* M. Zentilli and P.H. Reynolds. Mineralogical Association of Canada, pages 3-19.

Rudnick, R.L. and Gao, S.
2003: Composition of the continental crust, p/p. 1-64. *In* The Crust. *Edited by* R.L. Rudnick, Volume 3. *In* Treatise on Geochemistry. *Edited by* H.D. Holland and K.K. Turekian, Elsevier-Pergamon, Oxford.

Sandeman, H., McNicoll, V. and Evans, D.T.W.
2012: U–Pb geochronology and lithogeochemistry of the host rocks to the Reid gold deposit, Exploits Subzone – Mount Cormack Subzone boundary area, central Newfoundland. *In* Current Research. Newfoundland Department of Natural Resources, Geological Survey, Report 12-1, pages 85-102.

Silver, E.A. and Beutner, E.C.
1980: Melanges. Geology, Volume 8, pages 32-34.

Singer, B.S. and Pringle, M.S.
1996: Age and duration of the Matuyama-Brunhes geomagnetic polarity reversal from ^{40}Ar–^{39}Ar incremental heating analyses of lavas. Earth and Planetary Science Letters, Volume 139, pages 47-61.

Snee, L.W., Sutter, J.F. and Kelly, W.C.
1988: Thermochronology of economic mineral deposits; dating the stages of mineralization at Panasqueira, Portugal, by high-precision ^{40}Ar–^{39}Ar age spectrum techniques on muscovite. Economic Geology, Volume 83, pages 335-354.

Valverde-Vaquero, P., van Staal, C. R., McNicoll, V. and Dunning, G.R.
2006: Mid-Late Ordovician magmatism and metamor-

phism along the Gander margin in central Newfoundland. Journal of the Geological Society London, Volume 163, pages 347-362.

van Staal, C.R.
1994: Brunswick subduction complex in the Canadian Appalachians: record of the Late Ordovician to Late Silurian collision between Laurentia and the Gander margin of Avalon. Tectonics, Volume 13, pages 946-962.

van Staal, C.R., Dewey, J.F., Mac Niocaill, C. and McKerrow, W.S.
1998: The Cambrian-Silurian tectonic evolution of the Northern Appalachians and British Caledonides; history of a complex, west and southwest Pacific-type segment of Iapetus, *In* Lyell: the Past is the Key to the Present. *Edited by* D.J. Blundell and A.C. Scott. Geological Society Special Publication London, Volume 143, pages 199-242.

Van Staal, C.R., Valverde-Vaquero, P., Zagorevski, A., Pehrsson, S., Boutsma, S. and van Noorden, M.J.
2005: Geology, King George IV Lake, Newfoundland. Geological Survey of Canada, Open File 1165, scale 1:50,000.

Williams, H., Colman-Sadd, S.P. and Swinden, H.S.
1988. Tectonic–stratigraphic subdivisions of central Newfoundland. *In* Current Research, Part B. Geological Survey of Canada, Paper 88-1B, pages 91-98.

Williams, S.H.
1991: Graptolites from the Baie D'Espoir Group, south-central Newfoundland. *In* Current Research. Newfoundland Department of Natural Resources, Geological Survey, Report 91-1, pages 175-178.

Williams, S.H., Boyce, W.D. and Colman-Sadd, S.P.
1992: A new Lower Ordovician [Arenig] faunule from the Coy Pond Complex, central Newfoundland, and a refined understanding of the closure of the Iapetus Ocean. Canadian Journal of Earth Sciences, Volume 29, pages 2046-2057.

Zagorevski, A., van Staal, C. R., McNicoll, V. and Rogers, N.
2007: Upper Cambrian to Upper Ordovician peri-Gondwanan island arc activity in the Victoria Lake Super - group, central Newfoundland: tectonic development of the northern Ganderian margin. American Journal of Science, Volume 307, pages 339–370.